Mineralium Deposita (1999) 34: 673–696

ARTICLE

B. Mehrabi · B. W. D. Yardley · J. R. Cann

Sediment-hosted disseminated gold mineralisation at Zarshuran, NW Iran

Received: 10 December 1997 / Accepted: 5 March 1999

Abstract Mineralisation at the Zarshuran, NW Iran, occurs on the flank of an inlier of Precambrian rocks hosted in black silty calcareous and carbonaceous shale with interbedded dolomite and limestone varying in thickness from 5 to 60 m and extending along strike for approximately 5–6 km. Two major, steeply dipping sets of faults with distinct trends occur in the Zarshuran: (1) northwest (310–325) and (2) southwest (255–265). The main arsenic mineralisation occurs at the intersection of these faults. The mineral assemblage includes micron to angstrom-size gold, orpiment, realgar, stibnite, getchellite, cinnabar, thallium minerals, barite, Au-As-bearing pyrite, base metal sulphides and sulphosalts. Hydrothermal alteration features are developed in black shale and limestone around the mineralisation Types of alteration include: (1) decalcification, (2) silicification, (3) argillisation, (4) dolomitisation, (5) oxidation and acid leaching and (6) supergene alteration. The early stage of mineralisation involved removal of carbonates from the host rocks, followed by quartz precipitation. The main stage includes massive silicification associated with argillic alteration. In the late stage veining became more dominant and the main arsenic ore was deposited along fault cross cuts and gouge. These characteristics are typical of Carlin-type sediment-hosted disseminated gold deposits. The early stage of mineralisation contains only two-phase aqueous fluid inclusions. The main stage has two groups of three-phase CO_2-bearing inclusions with minor $CH_4 \pm N_2$, associated with high temperature, two-phase aqueous inclusions. During the late stage, fluids exhibit a wide range in composition, salinity and temperature, and CH_4 becomes the dominant carbonic fluid with minor CO_2 associated with a variety of two-phase aqueous fluid inclusions. The characteristics of fluids at the Zarshuran imply the presence of at least two separate fluids during mineralisation. The intersections of coexisting carbonic and aqueous inclusion isochores, together with stratigraphic and mineral stability evidence, indicate that mineralisation occurred at 945 ± 445 bar and 243 ± 59 °C, implying a depth for mineralisation of at least 3.8 ± 1.8 km (assuming a lithostatic pressure gradient). Fluid density fluctuations and the inferred depth of formation suggest that the mineralisation occurred at the transition between overpressured and normally pressured regimes. Geochronologic studies utilising K/Ar and Ar/Ar techniques on hydrothermal argillic alteration (whole rock and separated clay size fractions) and on volcanic rocks, indicates that mineralisation at Zarshuran formed at 14.2 ± 0.4 Ma, and was contemporaneous with nearby Miocene volcanic activity, 13.7 ± 2.9 Ma. It is proposed that mineralisation was the result of the infiltration of hydrothermal fluids containing a magmatic gas component, and that it was localised in the Zarshuran Unit because of the redox boundary that it provided and/or because it lay between an overpressured region at depth and a zone of circulating, hydrostatically pressured fluids above.

Introduction

The Zarshuran gold deposit is located at 36° 43.4′N 47° 08.2′E, 42 km north of the town of Takab in the West Azarbaijan province, NW Iran (Fig. 1). The Zarshuran deposit is well known for arsenic mining in Iran, orpiment and realgar having been worked for hundreds of years, but it is now of interest as a gold prospect. In this area, there are other deposits and prospects of As-Sb-Hg-Tl-Au mineralisation, which all seem epithermal in character and exhibit similar genetic features.

Editorial handling: E. Marcoux

B. Mehrabi[1] (✉) · B.W.D. Yardley · J.R. Cann
School of Earth Sciences, University of Leeds,
Leeds LS2 9JT, UK

Present address:
[1] Department of Geology, Tarbiat Moalem University,
Tehran, 15614-Iran
e-mail: Mehrabi@SABA.Emu.ac.ir, Fax +9821 6417358

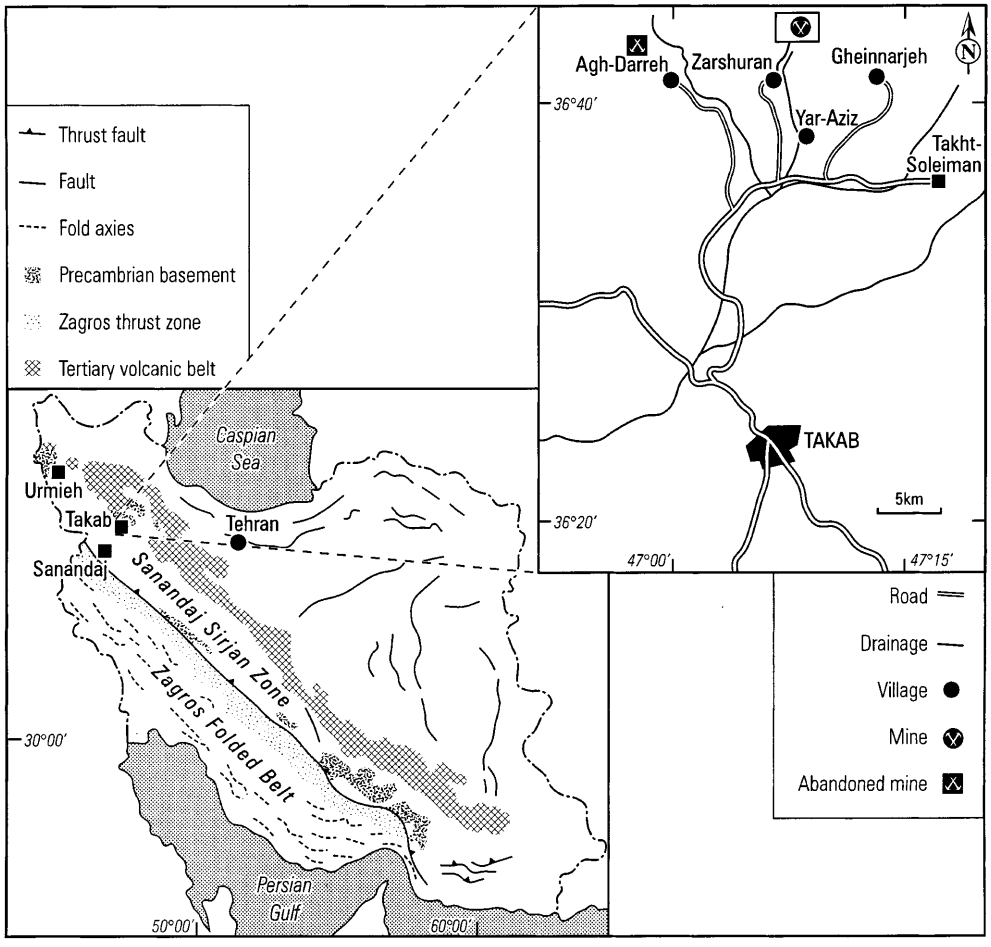

Fig. 1 Location map of the mineralised area, NW of Takab, and its relation to the Zagros subdivisions and the Tertiary volcanic belt according to Stocklin (1968). The *box* shown NE of Zarshuran in the detailed map is the area of the geological map (Fig. 2)

The Zarshuran deposit is the oldest arsenic mine in Iran and was certainly also mined for gold in ancient times. Large piles of rocks at four sites in drainage downstream along the Zarshuran river have been interpreted as product of alluvial mining (Mohajer et al. 1989; Samimi 1992). Old workings and trenches in the area seem to be the remains of ancient gold mining (Samimi 1992). Published reports regarding the specific geology of the Zarshuran deposit and other mineral prospects in the Takab area are very few. The first programme of regional geology in the Takab area was conducted by the Geological Survey of Iran in 1965 and the results of their studies were included in a 1:250 000 geological map and report for the Takab quadrangle (Alavi et al. 1982). Bariand (1962), Bariand et al. (1965), Bariand and Pelissier (1972), and Ghasemippur and Khoie (1971) studied the mineralogy of the arsenic mineralisation. Bariand et al. (1965) recognised "getchellite $AsSbS_3$" in the Zarshuran, which had been newly recognised in the Getchell mine, Nevada (Weissberg 1965). Mohajer et al. (1989) published the result of a preliminary reconnaissance for mercury in the area. Since 1990, the Ministry of Mines and Metals have conducted large-scale mapping of gold mineralisation in the area.

Geological setting

The Zarshuran mining area is a region of about 200 km^2 located in the Takab quadrangle of NW Iran (Fig. 1). Geologically it lies within the Alborz-Azarbaijan zone (Nabavi 1976), of the Alpine-Himalayan chain. A sedimentary sequence of more than 13 000 m in total thickness is exposed, mainly in the northern part of the Takab quadrangle, (Alavi et al. 1982), and ranges in age from Precambrian to Recent. Volcanic activity occurred in late Precambrian, Cretaceous, Eocene, Oligocene-Miocene and post Miocene times, and there are intrusives associated with several of these events.

The depositional sequence at Takab contains gaps and unconformities. Besides a long break in deposition from Silurian to Permian time, breaks also occur in the late Cambrian, early Jurassic, early Cretaceous, Oligocene-Miocene, Pliocene-Pleistocene and Quaternary sequences. Epicontinental and shallow marine rocks characterise the late Precambrian to Ordovician, Permian, Triassic and lower Jurassic formations while marine rocks constitute the middle and upper Jurassic, Cretaceous and Lower Miocene formations (Alavi et al. 1982). Terrestrial and continental beds are confined to the Oligocene, Middle and Upper Miocene and Pliocene.

Stratigraphy

According to Samimi (1992), the mining area is in a region of Precambrian metamorphic basement with late Precambrian car-

bonates and shales overlain by Cambro-Ordovician limestone and dolomite. Tertiary (Oligocene) rocks transgress with a basal conglomerate, marl, tuff and sandstone over these older rocks. Miocene volcanics, mainly andesite and rhyolite, disconformably overlie the Oligo-Miocene formations. A shallow dipping travertine of Quaternary age is exposed in several places in the area.

The Precambrian sequence, the *Iman Khan complex* (Mohajer et al. 1989), has been subdivided into three major units, (1) Iman Khan Unit, (2) Chaldagh Unit and (3) Zarshuran Unit by Samimi (1992).

The *Iman Khan Unit* outcrops in the core of the Iman Khan anticline, and comprises epidote schist, chlorite schist, and serpentine schist with intercalations of thin bedded marble and 1 to 5 mm thick veinlets of asbestos. The age of neither the metamorphism nor the protolith is known.

The *Chaldagh Unit* is a medium grey crystalline limestone up to 300 m thick, which unconformably overlies the Iman Khan Unit. In the lower part, it is micaceous and at the contact with the green schist, crumpled lenses of thin-bedded reddish shale outcrop. The supposed late Precambrian age is based solely on lithostratigraphy (Samimi 1992).

The *Zarshuran Unit*, the main host to the mineralisation, consists of black shale with intercalations of limestone and dolomite. The contact between the Zarshuran Unit and Chaldagh limestone is in part faulted, but appears conformable elsewhere. The Zarshuran Unit locally overlies the Iman Khan Unit directly (Fig. 2), and its age is not known with confidence. The Zarshuran Unit is commonly covered by debris from other units which make thickness measurements difficult, however in Mal Darrasi, the best exposed section, the thickness is about 130 m (Samimi 1992).

Rocks correlated with the *Qara Dash Formation* by Samimi (1992) occur on the southern flank of Iman Khan anticline, and conformably overly the Zarshuran Unit. They consist of rhyolitic tuff, quartz porphyry, rhyolite and sandstone and are followed by a 100 m succession of red shale and dolomite (correlated with the uppermost Precambrian Bayandor Formation by Samimi 1992).

This sequence is faulted against the *Soltanieh Formation* which spans the Precambrian-Cambrian boundary and overlies the Bayandor and Qara Dash Formation elsewhere. It is a yellow grey coloured dolomite, which contains chert nodules and lenses, with grey micaceous shales at intervals. The lower boundary of the Soltanieh Formation does not outcrop.

The *Barut Formation* gradually overlies the Soltanieh dolomite with intervals of red micaceous shales, grey dolomite and chert bands which may reach up to 1 m in thickness. It grades progressively up into the *Zaigun Formation*, which comprises 200 m of micaceous red and violet shale with thin layers of grey shale and

Fig. 2 Geological map of the Zarshuran deposit, NW Iran (modified after Samimi 1992)

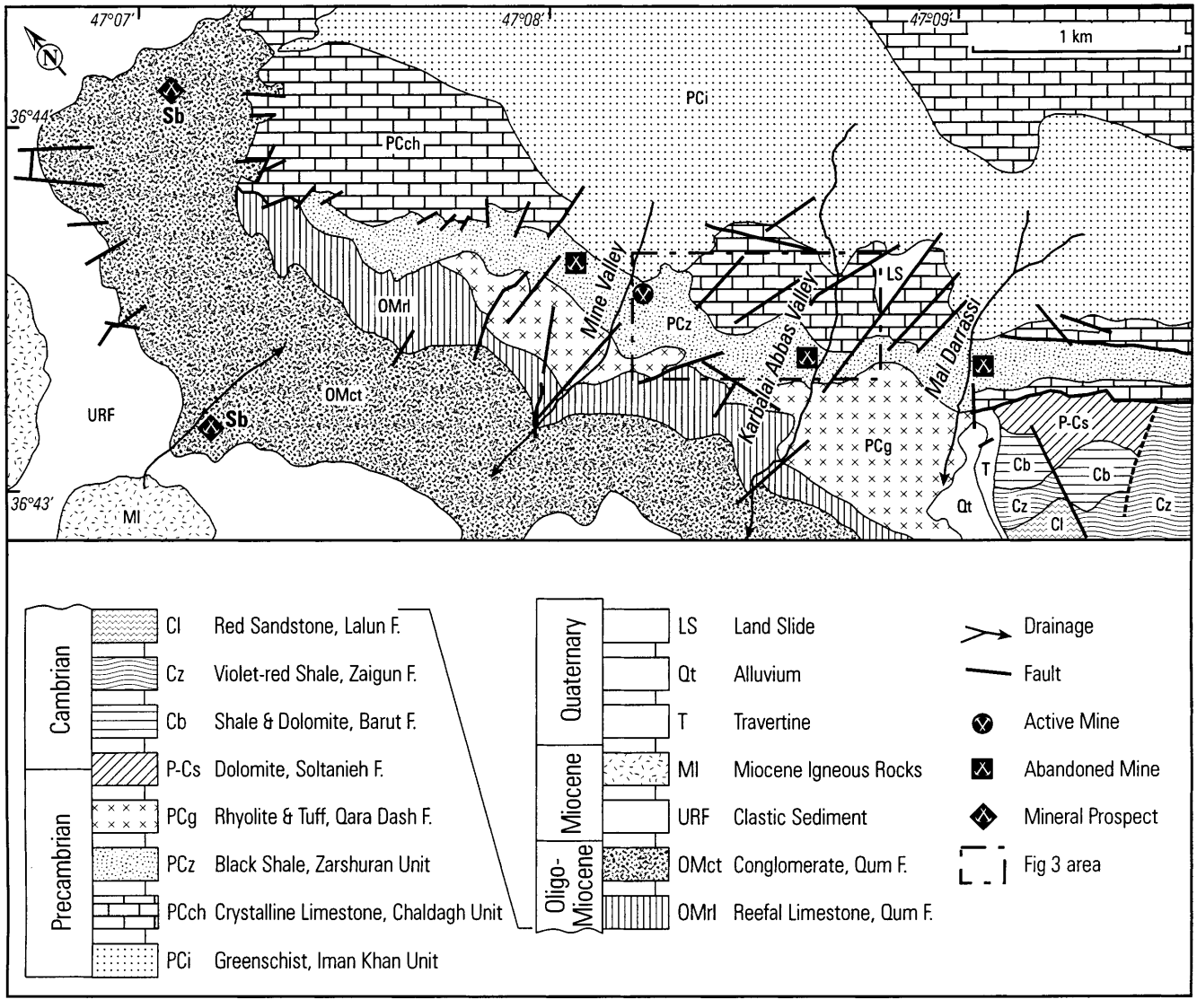

dolomite. The Palaeozoic sequence in the area is terminated by the *Lalun Formation* comprising red sandstone with white to pinkish quartzite at the top.

The basal Oligo-Miocene rocks of the *Qum Formation* are transgressive over the lower Palaeozoic and older rocks, with a basal conglomerate, followed by tuff, sandstone and reefal limestone up to 500 m thick (Samimi 1992). The basal conglomerate contains pebbles of acid volcanics, sandstone and shale (Mohajer et al. 1989). Associated fossils within the reefal limestone are early Miocene (Aquitanian) in age.

Clastic sediments of the *Upper Red Formation* (URF) overly the Qum Formation and contain sequences of red sandstone, claystone, marl and microconglomerate which formed under continental evaporitic conditions as a result of slow positive movement of the basin (Mohajer et al. 1989). In the mining area no evaporitic sediment have been reported. Clasts of volcanic rocks, mainly andesite, are the main constituent of URF conglomerates.

Late Miocene volcanic rocks disconformably overlie the URF in the mining area, and Mohajer et al. (1989) and Alavi et al. (1982) consider them younger than URF on a regional scale. The volcanic sequence begins with andesite and is followed by andesitic tuff, rhyolite and rhyolitic tuff. The presence of volcanic rocks in the URF conglomerate, and the disconformable volcanic sequence above it, indicate the continuation of periodic volcanic activity in the area through the Miocene.

Various types of surficial sedimentary deposits of Quaternary age are present in the area. Most common are unconsolidated stream alluvium and slope wash. Shallow dipping creamy white to light grey travertine of Quaternary age is exposed in few places adjacent to the Zarshuran mine. These probably resulted from hot spring activity.

Structure

The dominant structure at the Zarshuran deposit is the Iman Khan anticline. This structure is about 7 km long and 2 km wide, with a NW-SE trend. The dip of the south west limb is 35–50° and that of the northern one is 45–70°. Successively younger Cambro-Ordovician rocks outcrop toward the south of the anticline. The sequence is truncated by a high angle reverse fault at the northeast end of the anticline which juxtaposes late Precambrian and Oligo-Miocene sequences.

Poor surface exposure, local changes in the attitude of the beds over short distances and the covering of alluvial deposits make it difficult to recognise faults in Zarshuran, however two major sets of faults with distinct trends occur at the Zarshuran mine: (1) northwest (310–325) and (2) southwest (255–265). The northwest set comprises two parallel faults with a 300 m-long surface exposure length (Fig. 3). Of these, the northern fault has an important role in the mineralisation, and patches and lenses of brecciated quartz occur along it. Its surface trace is marked by the juxtaposition of the Zarshuran and Chaldagh Units west of the mining area. The southwest trending faults occupy valleys in Zarshuran and the thickness of the mineralised zone increases at the intersection of the two sets of faults.

Mineralisation in the vicinity of the Zarshuran Mine

Within the Zarshuran mining area, there are active mines as well as several sites of ancient mining and mineral prospects. Zarshuran and Agh Darreh (Fig. 1) are the two main ore deposits in NW Takab. Mineralisation at Zarshuran occurs at the contact between Precambrian limestone and black shale. The age of the host rock is not known for sure, although lithostratigraphy suggests late Precambrian.

Agh Darreh comprises an inlier of Precambrian granite and Cambrian red sandstone, and is overlain by Miocene rocks, consisting of tuffaceous volcanics, limestones and clastic sediments. Mineralisation occurs at two levels in the Oligo-Miocene sequence, (Qum Formation). The lower site is above the Tertiary basal conglomerate and contains antimony ore hosted by grey to black shale and marl. The upper site is a 3–8 m thick unit of very fine grained acid tuff sandwiched between brown limestone. Preliminary studies suggest that most of the gold mineralisation is in the upper site.

Other mineral prospects in the area include Baldir Ghanee and Bekhir Bolaghee which are hosted by the Oligo-Miocene sequence, and various quartz veins which are emplaced in the upper Miocene volcanic series.

Sampling

Detailed field work has been carried out at different scales at the Zarshuran mine, at three other smaller deposits and in the Miocene volcanic rocks. Emphasis was placed at Zarshuran on systematic sampling from outcrops, tunnels, trenches and visual logging and sampling from six bore holes (Fig. 3).

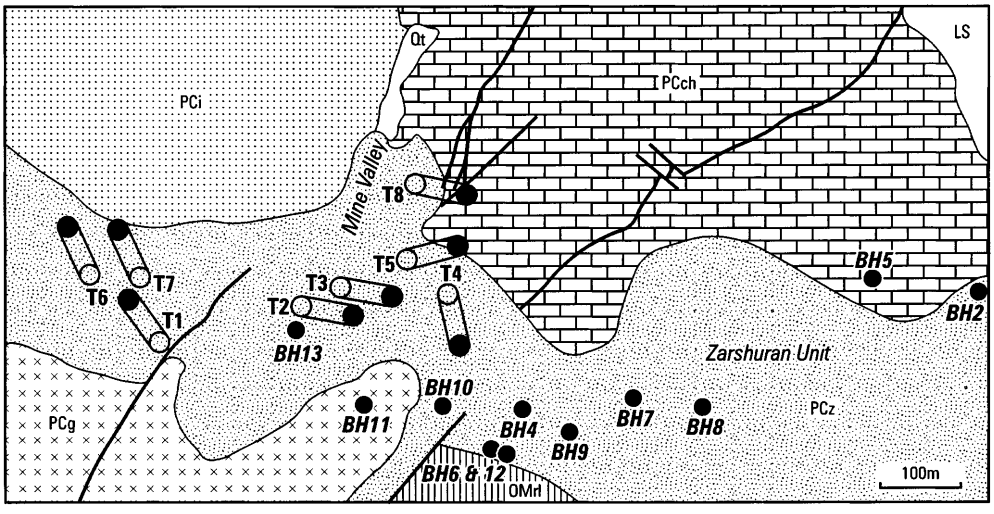

Fig. 3 Location map of tunnels (*T*) and bore holes (*BH*) at the Zarshuran mine. For key see Fig. 2

About 70 polished blocks, polished thin sections and grain mounts from unaltered host rocks, mineralised and altered zones and 30 samples of the Miocene volcanics were examined by conventional petrographic and mineralogic methods. In addition most polished preparations were investigated by scanning electron microscope (SEM), using an energy dispersive analyser for mineral identification and quantitative analysis by electron microprobe (EMP).

About 20 crushed samples were split and a split of each was subjected to X-ray diffraction analysis (XRD), then suspended in water and centrifuged to separate the less than 2 μm fraction. The resulting clay size particles were air dried, glycolated at 60 °C, heated incrementally to 300 °C and 500 °C and X-rayed at each step for clay mineral identification.

A split of the powdered material was analysed for major and trace element by Inductively Coupled Plasma Atomic Emission Spectrometry (ICP-AES). Twenty five samples from different ore types, alteration zones and veins were analysed for gold by fire assay and for As, Sb, Hg, Ag and Tl by atomic absorption spectroscopy (AAS) (Table 1). Total organic carbon of the powder was analysed by the rock-eval method (Table 2).

Table 1 Partial chemical analyses of host, mineralised and altered rocks from the Zarshuran deposit. Gold measured by fire assay method, others by AAS. Detection limits; Au (0.01 ppm), As (20 ppm), Ag (5 ppm), Sb (2 ppm), Te (5 ppm) and Tl (5 ppm)

Sample number	Sample description	Ore type	Au (ppm)	As (%)	Ag (ppm)	Sb (%) + (ppm)	Te (ppm)	Tl (ppm)
56931	Jasperoid	Silicic	13.00	4.1	15	0.30	35	32
56936	Silicified shale	Silicic	3.8	0.22	35	0.14	5	64
56937	Nearly pure orpiment	Arsenical	1.08	62	nd	1.04	220	8
57523	Microcrystalline quartz		0.01	0.02	nd	0.00	nd	nd
57528	Fl. vein in black shale	Normal	0.33	2.50	840	3.90	15	34
57532	Fl. ± Sph. vein in black shale	Carbonaceous	0.58	0.80	65	0.80	20	34
57534	Dolomitised shale		0.01	0.01	nd	30^{+}	nd	nd
57535	Black organic-rich shale	Carbonaceous	19.00	3.90	nd	0.01	5	70
57536	Calcareous shale		0.04	0.02	nd	4^{+}	nd	nd
57539	Black organic-rich shale	Carbonaceous	0.18	0.02	nd	8^{+}	nd	2
57542	Black organic-rich shale	Carbonaceous	0.76	0.03	nd	22^{+}	nd	10
57543	Calcareous shale		0.03	0.20	nd	20^{+}	nd	18
57545	Black mineralised shale	Arsenical	0.06	8.20	nd	10^{+}	nd	nd
57547	Black carbonaceous shale	Carbonaceous	1.45	2.95	4800	5.80	30	66
57549	Mineralised black shale	Pyritic	1.45	0.07	nd	0.01	nd	12
57847	Microcrytalline orpiment	Arsenical	110	60	5	20^{+}	85	480
BH9-71.5	Silicified black shale	Normal	0.54	1.20	135	1.45	30	46
BH9-80.6	Host rock		nd	0.01	nd	8^{+}	nd	nd
BH9-125	Black shale	Normal	0.48	0.02	nd	4^{+}	nd	nd
BH9-223	Powdery limestone		0.94	2.40	nd	0.02	10	nd
BH10-77	Quartz vein	Silicic	0.96	0.84	nd	0.22	10	4
BH10-127	Black organic-rich shale	Carbonaceous	2.05	0.06	nd	24^{+}	nd	10
BH10-265	Massive carbonate	Normal	0.13	0.01	nd	4^{+}	nd	nd
BH10-286	Green schist		0.01	0.06	nd	2^{+}	nd	nd
T9-50W	Weathered shale	Pyritic	36	18	70	5.50	1350	80
P9830*	Carbonaceous rock	Carbonaceous	0.41	0.02	nd	12^{+}	nm	nm
P9831*	Leached rock		0.07	0.40	nd	17^{+}	nm	nm
P9832*	Altered black shale	Normal	0.98	0.21	nd	28^{+}	nm	nm
P9833*	Schist with quartz vein	Silicic	0.30	0.03	nd	10^{+}	nm	nm
P9834*	Black organic-rich shale	Carbonaceous	0.75	0.38	nd	0.02	nm	nm
P9835*	Black shale		0.07	0.09	nd	43^{+}	nm	nm
P9836*	Weathered black shale		0.16	0.14	nd	36^{+}	nm	nm
P9837*	Mineralised black shale	Pyritic	6.21	0.90	nd	0.10	nm	nm
P9838*	Black shale (waste)	Arsenical	0.22	1.57	nd	0.01	nm	nm
P9839*	Black shale (waste)	Arsenical	6.16	2.61	nd	0.14	nm	nm
P9840*	Black organic-rich shale	Carbonaceous	0.05	0.19	nd	19^{+}	nm	nm
P9841*	Calcareous shale	Normal	3.18	1.58	nd	0.50	nm	nm
P9842*	Siliceous bed in limestone	Silicic	2.36	0.53	12	0.39	nm	nm
P9843*	Chert in limestone	Silicic	3.84	0.20	nd	0.34	nm	nm
P9844*	Black shale	Normal	0.41	0.12	nd	0.01	nm	nm
P9845*	Quartz vein	Silicic ore	1.08	0.06	nd	0.03	nm	nm
P9846*	Brecciated gossan		0.04	0.01	nd	10^{+}	nm	nm
P9847*	Silicified and leached rock		0.05	0.02	nd	0.01	nm	nm
P9848*	Fe rich carbonate		0.01	0.01	nd	10^{+}	nm	nm
P9849*	Altered carbonate	Normal	0.65	0.10	nd	28^{+}	nm	nm
P9850*	Carbonate-shale contact	Normal	0.14	0.97	nd	0.04	nm	nm
P9851*	Black shale	Normal	0.60	0.58	11	0.06	nm	nm
P9852*	Black shale	Normal	0.91	2.04	nd	0.06	nm	nm
P9853*	Mineralised black shale	Arsenical	1.43	2.24	11	0.10	nm	nm
P9854*	Mineralised black shale	Pyritic	7.37	2.15	nd	0.11	nm	nm
P9855*	Silicic rock	Silicic	1.39	1.90	nd	0.12	nm	nm
P9856*	Weathered mineralised shale	Arsenical	1.33	3.89	nd	0.90	nm	nm

nd: not detected; nm: not measured; * Iranian Ministry of Mines and Metals, internal report by BHP, Australia

Table 2 Total organic carbon contents of host and mineralised rocks

Sample	Sample type	TOC (%)	Hand specimen description	Major minerals (> 5%)	Minor minerals
T5-DP	Silicic ore	0.97[a]	Black silicified shale	Quartz and orpiment	Barite, sphalerite, galena, pyrite, stibnite and covellite
BH2N	Weathered host rock	1.35[a]	Weathered dark grey to brown calcareous shale	Quartz and calcite	Dolomite, sericite and iron hydroxides
T7-DP	Silicic ore	1.40[a]	Black mineralised shale	Quartz and orpiment	Clay minerals and pyrite
T8-DP	Arsenical ore	1.27[a]	Dark grey mineralised siltstone	Quartz and orpiment	Realgar, sericite, pyrite, stibnite and sphalerite
T8-DL68	Arsenical ore	0.91[a]	Dark grey silicified shale with arsenic mineralisation	Quartz and orpiment	Sericite, sphalerite, pyrite galena, stibnite, realgar, geocronite and cinnabar
T9-16E	Normal ore	0.41[a]	Dark grey calcareous shale with Quartz and Pyrite veinlets	Quartz, calcite, dolomite and clay minerals	Sphalerite, pyrite, marcasite, galena, barite, chalcopyrite, cinnabar, xenotime, monazite and lautite
T9-62W	Weathered silicic ore	0.63[a]	Dark grey silicic rock with vuggy structure	Quartz and clay minerals	Pyrite, realgar, orpiment and iron hydroxides
56931	Weathered silicic ore	1.49[a] 1.54 (1.38)[b]	Vuggy black silicified rock	Quartz	Pyrite, orpiment, scorodite, sphalerite, cinnabar and iron hydroxides
56936	Silicic ore	0.57[a] 0.38	Dark grey silicified rocks with base metal sulphides	Quartz and sphalerite	Orpiment realgar, galena, pyrite, stibnite and cinnabar
57528	Fluorite veins in normal ore	0.58	Black shale with fluorite ± Quartz ± Sphalerite veins	Quartz, clay minerals, fluorite and sphalerite	Pyrite, As-Sb sulphides and sulphosalts
57532	Carbonaceous ore with fluorite vein	2.44	Black shale with fluorite ± Quartz ± Sphalerite veins	Quartz, sphalerite, clay minerals and fluorite	As-Sb-Pb-Zn sulphosalts, pyrite, rutile and uranium oxide
57534	Dolomitised calcareous pyritic shale	1.03	Grey calcareous shale with carbonates grains up to 1 cm, collapsed structure	Calcite, dolomite and quartz	Pyrite, apatite, monazite and zircon
57535	Carbonaceous ore	4.80	Black shale with Orpiment patches	Quartz, dolomite, calcite and mica	Organic materials, pyrite, sphalerite, rutile, apatite, zircon, monazite and uranium oxide
57536	Carbonaceous shale	4.85 (4.38)[b]	Carbonaceous shale and calcareous shale contact	Dolomite, calcite and quartz	Pyrite, mica and rutile
57539	Carbonaceous ore	8.65 (8.04)[b]	Calcareous carbonaceous shale with calcite grains (5mm)	Calcite, quartz and clay minerals	Pyrite, sphalerite, rutile and zircon
57542	Carbonaceous ore	12.79 (14.50)[b]	Black carbonaceous shale	Quartz, organic material and clay minerals	Pyrite, As-Sb-Fe-Pb-Zn sulphides and sulphosalts and apatite
57547	Carbonaceous ore	2.95	Black carbonaceous shale with fluorite ± Quartz ± Sphalerite veins	Quartz, fluorite and sphalerite	Pyrite, stibnite, As-Sb-Pb-Fe sulphides and sulphosalts
57549	Pyritic ore	1.48	Dark grey silicified shale with carbonaceous laminae (up to 3 mm)	Quartz, clay minerals, calcite and dolomite	Pyrite, stibnite, sphalerite, apatite, rutile and monazite
BH9-71.5	Normal ore	1.12	Dark grey shale	Quartz and clay minerals	Pyrite, fluorite, stibnite and rutile
BH9-80.6	Host rock	1.2	Calcareous shale	Calcite, quartz and clay minerals	Pyrite
BH9-125	Normal ore	1.2	Altered calcareous shale with collapsed structure	Calcite, quartz and clay minerals	Pyrite and orpiment
BH10-41	Calcareous shale	0.09	Dark grey silicic shale with As and Hg sulphides and calcite veinlets	Quartz, calcite and clay minerals	Orpiment, realgar, cinnabar, stibnite and pyrite
BH10-127	Carbonaceous ore	4.26	Black calcareous shale	Quartz and clay minerals	Calcite and pyrite

[a] Measured by rock evaluation method
[b] Duplicate

Following petrographic studies of 30 wafers prepared from the different stages of mineralisation, 12 samples were chosen for fluid inclusion micro thermometry and crush leach analysis. The gas species in fluid inclusions from two samples were analysed by laser Raman spectroscopy. Seventeen samples, whole rocks and separate phases, from mineralised rock and volcanic rocks have been dated by K/Ar or Ar/Ar method.

Ore body geometry

The gold and arsenic mineralisation at the Zarshuran deposit is semi-conformable within the Zarshuran Unit along a strike length of 1 km, and dips approximately 35–50°SW. The Zarshuran Unit is exposed for about 5 km and mineralisation has been reported to occur to different degrees in different parts of this unit (Samimi 1992). The thickness of the mineralised zone varies between 5–60 m with an average of 15–20 m. The main arsenic mineralisation is in the form of a series of anastamosing pods, lenses and veins; the average thickness of the lenses is about 3 m.

Characteristics of the host rock

In the Zarshuran deposit, mineralisation occurs in the upper part of the Chaldagh Limestone and in the Zarshuran Black Shale Unit. The Zarshuran Black Shale Unit is the main host rock, and its best exposure is in the Mal-Darrassi valley, 1800 m southeast of the arsenic mine. The Zarshuran Unit outcrops in a zone about 5 to 6 km long and up to 100 m wide along the southeast flank of the Iman Khan anticline (Samimi 1992). It consists of alternating carbonates and clastic sediments.

The upper part of the massive Chaldagh limestone has been transformed to a porous powdery limestone as a result of hydrothermal alteration. This transformation has been observed in all bore holes and is best exposed along a trench dug at the top of adit 5 on the south flank of the Zarshuran valley.

Three main types of beds can be distinguished in the host rock; (1) laminated argillaceous limestone with interbedded calcareous siltstone which contains organic material, (2) relatively massive carbonate and (3) calcareous siltstone and very fine grained mature sandstone with arenaceous texture, in which the main detrital mineral is quartz.

A planar fabric, oriented parallel to the stratification, results in millimetre to centimetre thick laminated beds in the main host rock. The interbedded coarser grained calcareous siltstones contain more quartz and less clay than adjacent laminated beds. The boundary between the siltstone and the very fine grained sandstone is gradual. These coarser clastic beds apparently were important stratiform conduits for hydrothermal fluid as a consequence of higher permeabilities than adjacent beds.

Detailed petrographic, mineralogical and X-ray diffraction studies of the main host rocks show that the contents of the major constituents (calcite, quartz, dolomite and clay minerals) vary widely between individual samples. The typical initial mineralogy of the host rock is 30–50% calcite, 30–40% quartz, 5% dolomite and 5–15% clay-mica. Illite and sericite are the major clay minerals. Detrital potassium feldspar and plagioclase on average comprise less than 1% of the host rocks. Minor constituents, collectively less than 3%, include pyrite, monazite, rutile, zircon and carbonaceous materials. The carbonaceous material and clay minerals are commonly admixed and are concentrated in millimetre scale laminations.

Alteration

Hydrothermal alteration features are developed in the Zarshuran Unit and the Chaldagh limestone. The intensity of alteration is locally variable and ranges from weak to intense. Alteration at the Zarshuran gold deposits is divided into six categories, mainly based on mineralogy. These are (1) decalcification, (2) silicification, (3) potassic argillisation, (4) dolomitisation, (5) minor oxidation and acid leaching and (6) supergene alteration. There are apparently no systematic relationships between the alteration types, except as noted later. Silicification is the dominant type of alteration in other prospects in the area. Prominent oxidation has not been observed in Zarshuran.

Decalcification Decalcification involves the removal of calcite and dolomite from the sedimentary host rock by weakly acidic solutions. In the Zarshuran, decalcification affected both the Chaldagh limestone and the Zarshuran Unit. Massive Chaldagh limestone in contact with the Zarshuran Unit has been altered to loose powdery and porous limestone. Decalcification has been recorded in all of the exploration bore holes at Zarshuran. The importance of early hypogene alteration is to increase porosity and permeability of the host rocks and thus make them more favourable for mineralisation. The process of hypogene hydrothermal alteration of carbonate-rich hosts invariably begins with decalcification, which is characteristic of sedimentary hosted precious metal deposits (Radtke 1985; Bagby and Berger 1985; Percival et al. 1988; Berger and Bagby 1991).

Silicification Extensive hydrothermal silicification has also occurred in the Zarshuran Unit. The intensity of silicification varies from weak to total, jasperoid, replacement of calcareous rocks. Replacement of carbonate with quartz has locally altered the Zarshuran calcareous silty shale to noncalcareous, carbonaceous "siltstone".

The silicified rocks are products of the introduction of hydrothermal silica and replacement along faults and fracture zones of varying orientations. Silica-bearing fluids also moved from fractured zones outward along

stratigraphic horizons, resulting in both weak pervasive silicification and micro-stockworks in fracture zones.

The jasperoids are grey to black in colour and consist of fine-grained microcrystalline quartz that obliterates the textures of the pre-existing calcareous rocks. Features such as breccia textures, quartz veins and veinlets, are common and there is evidence for more than one episode of jasperoid formation. Jasperoids consist of greater than 95% quartz and the microcrystalline quartz normally contains small inclusions of calcite. Jasperoids normally have a porous texture indicating that precipitated quartz occupies less volume than that of removed carbonates.

Disseminated sulphides are present in the jasperoids and include stoichiometric pyrite, arsenian pyrite, orpiment, stibnite and rare arsenopyrite. Stoichiometric pyrite occurs as cubes or framboids less than 50 microns in size. Arsenian pyrite contained 0.5–3.4 wt.% As and is normally overgrown on stoichiometric pyrite or as disseminated grains.

The early jasperoids are more porous and contain less sulphide, mainly pyrite, than jasperoids formed during the main stage of hydrothermal activity. The main stage jasperoids contain arsenic, antimony and minor zinc sulphides in addition to pyrite and arsenian pyrite. The presence of 3–5 micron size metallic gold in jasperoids was reported by Mohajer et al. (1989), but no trace has been detected by either microscopy or SEM in the present study.

Potassic-argillic alteration The potassic-argillic alteration, which is pervasive throughout the Zarshuran deposit, is areally extensive and is of varying intensity. Argillic alteration is intimately associated with the gold mineralisation and is evident in all mineralised rocks and unoxidised ore types formed during the main hydrothermal stage.

Calcareous rocks which have been affected by potassic-argillic alteration, including those that have been mineralised, closely resemble the fresh unaltered rocks, with no pronounced colour changes, but contain up to 4% clays.

The moderately to intensely argillised rocks consist of varying proportions of fine-grained clays (sericite, illite and kaolinite have been identified by XRD), quartz, calcite, gypsum, sulphides (pyrite, orpiment and realgar) and As-Sb sulphosalts.

Dolomitisation A mixture of Fe and Mn-bearing dolomite (SEM data) was precipitated after the argillic alteration in both shale and limestone hosts. The hydrothermal dolomite formed during dolomitisation is fine grained and shows patchy zonation in back scattered electron (BSE) mode. Generally, late dolomite is Fe-Mn bearing and heterogeneous in comparison to host rock dolomite which is low in Fe and Mn and homogenous. In some cases, hydrothermal dolomite forms a halo around relict Fe-Mn-free dolomite of host rocks.

Dolomitisation is weakly developed at the Zarshuran deposit, and probably formed at a late stage of hydrothermal activity. It is sometimes difficult to confirm whether dolomite-rich rocks are due to hydrothermal dolomitisation with new dolomite growth, or to removal of calcite from original dolomite rocks by low-pH hydrothermal fluids. The main sulphide associated with dolomite is pyrite.

Oxidation and acid leaching Oxidation and acid leaching are not widespread at Zarshuran and are restricted to the local development of bleached rocks in shattered zones and rarely along stratigraphic horizons. Stratigraphically controlled acid leaching observed in BH8 and BH12 (Fig. 3) is up to 3 m in thickness. The degrees of acid leaching alteration may be classified as weak, moderate, or intense based on relative amounts of carbonate removal.

The conversion of pyrite to Fe oxides, and the oxidation of small amounts of organic carbon have resulted in buff-tan rocks, in contrast to the black-grey unoxidised ore and host rocks. The oxidised rock contains mainly quartz and a mixture of clay minerals, and has a very low calcite content. Small amounts of anhydrite, jarosite and various secondary iron minerals occur as accessory minerals. Visual evidence for oxidation hinges largely on pyrite stability and the presence or absence of small amounts of organic carbon.

The oxidation and acid leaching are related to deep weathering (see Bakken and Einaudi 1986; Kuehn and Rose 1992) rather than hypogene hydrothermal processes because: (1) most of the oxidation is localised adjacent to fractures and veinlets, (2) the oxidised rock contains amorphous goethitic to limonitic Fe oxides rather than hematite, (3) Fe oxides have replaced pyrite and (4) similar characteristics (texture and mineralogy) are present in both near-surface altered rocks and deeper oxidised rocks. However stratigraphically controlled, bleached rock may still be the result of hypogene acid leaching.

Supergene alteration Supergene alteration is weakly developed in Zarshuran, and is located in fractured zones where it reaches a maximum thicknesses of 3 m. In localised intensive supergene alteration, the black mineralised rock or host rock has changed to a brown to brownish-red colour in which the main minerals are scorodite and iron hydroxides. The effect of weathering is similar in both noncalcareous and calcareous rocks. A sample analysed for gold from the supergene altered rock (sample T9-50W, Table 1) shows a higher gold concentration and may have been enriched by supergene processes.

Gold mineralisation

The Zarshuran district is a historic arsenic mining centre, and until now gold exploration has only been carried

out on a small scale in the vicinity of the orpiment mine. The preliminary results obtained from trenching, bore holes and soil geochemistry suggest that gold occurs in a zone about 1 km long, with an average thickness of 15 m. Surface sampling indicates 2 ppm gold on average (Taddaion 1991), although underground sampling has yielded much higher values locally. Without a lot more exploration, a realistic estimate of tonnage and grade is impossible. A probable reserve of 2.5 million tonnes ore with 10 ppm gold estimated by Samimi (1992) looks very optimistic.

Gold values ranging from 9 ppm (Bariand and Pelissier 1972) to 33.26 ppm (Kyazimov 1993) have been reported for ores from Zarshuran. The reasons for the large variation include lack of detailed mineralogic and petrographic investigation and classification of gold ore.

Unoxidised ores at the Zarshuran contain quartz, calcite, dolomite, clay minerals (major illite and sericite and minor kaolinite), carbonaceous material, As, Sb, Hg, Au, Pb and Zn minerals, with the same accessory minerals found in the unmineralised host rocks. The unoxidised ore can be divided into five types on the basis of mineral content and association of gold; (1) silicic ore, (2) arsenical ore, (3) pyritic ore, (4) carbonaceous ore and (5) normal ore.

Silicic ore

This is characterised by high silica contents, very small amounts of remnant carbonates and low sulphide content. The ore is dark grey to black and normally contains 85–95% quartz, 2–5% clay minerals, 1–5% calcite and dolomite and smaller amounts of pyrite, arsenian pyrite, arsenic and antimony sulphides and carbonaceous material. Hydrothermal silica has generally replaced most of the carbonates in the host rocks. In silicic ore, quartz is microcrystalline and sometimes has a micro-stockwork texture. The main sulphide mineral in silicic ore is pyrite, which is very fine grained, subhedral to euhedral, and scattered throughout the quartz matrix. It comprises 1–3% of the ore. Other sulphides identified include orpiment, stibnite, realgar, sphalerite, galena, chalcopyrite and lautite. All these minerals are very fine grained and disseminated, with abundances invariably less than 1%. Micron size metallic gold has been reported by Mohajer et al. (1989), was not found in this study; most of the gold in this type of ore probably occurs within pyrite and is detectable only by chemical analysis (Table 1).

Arsenical ore

This occurs mainly at the intersection between two sets of dominant faults at the three valleys in the Zarshuran mine. Irregular masses and lenses of yellow-orange colour arsenic sulphides, which account for most of the arsenic in the rock, are prominent against the black host rock. The ore contains arsenic sulphides in quantities from a few percent up to more than 40% (commercial arsenic ore). The main arsenic mineral is orpiment, and this is associated with lesser amounts of realgar and various sulphosalts and sulphoarsenides. The main gangue mineral is quartz. Small subhedral to euhedral pyrite occurs as inclusions in quartz and orpiment. The arsenic sulphides occur as very small veinlets up to mineable lenses, and show a variety of textures and crystallinity, including open space filling, brecciated, colloform, botryoidal and radial textures.

Gold is occasionally observed in arsenical ore, occurring as micrometer size metallic gold in thin films around orpiment and realgar. It is probably also present substituting in the structure of arsenic minerals. One sample (57847), of fine grained microcrystalline arsenical ore with abundant mosaic-texture realgar, contains 2–20 micron size native gold. Pyrite associated with arsenical ore shows detectable amounts of gold by electron microprobe.

Carbonaceous ore

This is dark grey to black in colour and contains abnormally large amounts of organic carbon. The term "carbonaceous ore" was introduced by Radtke (1985) for the Carlin deposit, and has been used previously for metallurgical purposes.

The ore occurs as thin bedded, alternating dark grey and black laminae, to dense black and unlaminated rocks. Carbonaceous ore normally varies from black thin-bedded and laminated dense and unlaminated rocks containing black amorphous organic material. The content of organic carbon in carbonaceous ore is commonly more than 1% and locally as high as 13% (Table 2). Otherwise, most of the carbonaceous ore resembles the normal ore except for a slightly lower content of remnant calcite. Corroded rhombs of dolomite and angular quartz grains are dispersed throughout a matrix composed of clay, fine-grained quartz, dolomite and carbonaceous material. Most of the fine-grained calcite in the matrix has been dissolved out, and the voids have been filled by carbonaceous material. Remnants of the calcite and some of the dolomite have been replaced by hydrothermal quartz, pyrite and arsenic minerals. In addition to the carbonaceous material in the matrix, it also occurs in small veinlets, commonly parallel to bedding.

The alternating grey and black laminae of the carbonaceous ore reflect differences in mineralogy and chemical composition. The grey laminae are composed of sub-angular detrital quartz grains and dolomite rhombs in a clay matrix with fine-grained calcite and quartz. The black laminae contain quartz grains, corroded dolomite rhombs and clay minerals with small amounts of remnant calcite. In general, grey laminae contain more

calcite and less carbonaceous material in comparison to black laminae, and the main carbonate in the black laminae is dolomite.

Pyrite is the most abundant sulphide mineral in the carbonaceous ore and occurs in both cubic and framboidal forms. By comparison, other sulphide and sulphosalt minerals are sparse and occur randomly distributed throughout the ore. They include orpiment, stibnite, realgar, galena, sphalerite and a few sulphosalts and sulphoarsenides of Sb, Zn, Cu, Fe and/or Ag, which have not been examined in detail. These minerals are very heterogeneous, and in backscattered electron images a range of compositions can be observed in a single grain. In two samples of carbonaceous ore, 3–5 micron size uranium oxide and thorium silicate have been recognised.

Pyritic ore

This is medium to dark grey and commonly contains visible pyrite in hand specimen. Pyrite occurs in two forms (1) as bands or oriented patches ranging from few millimetres up to a centimetre thick and (2) disseminated throughout the ore. Most of the pyrite occurs as subhedral to euhedral grains, with a very small amount of subrounded and framboidal grains.

The pyritic ore normally consists of relatively small amounts of remnant carbonate and clay minerals, in a matrix mainly composed of silt-size subangular detrital quartz grains. Sulphide minerals other than pyrite are uncommon, but sparse arsenic and antimony sulphides are scattered randomly throughout it. Metallic gold grains have not been found in pyritic ore but Bariand and Pelissier (1972) reported 250 ppm gold in a pyrite rich sample.

Normal gold ore

This appears similar to unmineralised black calcareous shale. It is dark grey in colour, and is mainly composed of carbonate, quartz, clay minerals and carbonaceous matter. The main hydrothermal features are the replacement of carbonate, with introduction of silica and the overgrowth of quartz and pyrite. In addition to the diagenetic pyrite inherited from the original sediment, hydrothermal pyrite occurs as disseminated subhedral grains and framboids in the matrix.

Stoichiometric pyrite and arsenian pyrite are the predominant sulphides in the ore, with the minor minerals comprising arsenic and antimony sulphides. Diffractograms of normal gold ore indicate the presence of quartz, calcite, dolomite, muscovite (sericite), illite and gypsum. In comparison to the carbonaceous gold ore, normal gold ore contains less organic matter and more carbonates. Native gold has not been found in normal ore and gold is associated with pyrite and arsenian pyrite. The highest gold value recorded from the normal ore in this study is 4 ppm.

Distribution of Au, As, Sb, Ag, Te and Tl in different ore types

Metallic gold is very rare at the Zarshuran deposit and most of the gold is detectable by chemical analysis only. Table 1 shows the result of chemical analysis of unmineralised host rock, altered and mineralised samples from the Zarshuran deposit. The high gold values in samples 57847 and 57535 reflect the presence of metallic gold inclusions, while sample 9-50W is weathered pyritic ore in which pyrite and arsenian pyrite have altered to iron-arsenic hydroxides, and the high gold grade may reflect supergene enrichment.

The average of Au, As and Sb concentrations in the different ore types (Table 3) shows that pyritic and arsenical ores contain the highest value for gold. The strong correlation between As and Au (Table 4 and Fig. 4) and the high gold values in arsenical and pyritic ores (Table 1) confirm the results of mineralogical studies (Mehrabi 1997), indicating that gold is associated mainly with orpiment-realgar and pyrite-arsenian pyrite. The positive correlation between As and Sb (Table 4) also shows the association of As and Sb as coexisting sulphide minerals and/or in solid solution.

In contrast to many other types of gold deposits, the Zarshuran contains little silver. However high silver values were recorded in samples 57528 and 57549, and reflect the presence of Ag-rich stibnite. SEM analysis indicates that Zarshuran stibnite contains both inclusions of native silver, 2–5 μm in size, and patchy areas of Ag-enrichment (BSE mode).

Tellurium is detected in a few samples from the Zarshuran deposit (Table 1). No telluride minerals have been identified despite the very high tellurium value for sample T9-50W. High tellurium values in samples 56937 and 57547 (Table 1) suggest an association of tellurium

Table 3 The average concentrations of Au, As and Sb in different ore types at the Zarshuran deposit

Element	Ore type				
	Siliceous	Arsenical	Normal	Pyritic	Carbonaceous
Gold (Au ppm)	3.34	26.7 (8.01[a])	0.72	12.7	3.08
Arsenic (As %)	0.98	26.68	0.90	5.28	0.94
Antimony (Sb %)	0.19	0.80	0.62	1.43	0.73

[a] Excluding very high results

Table 4 Linear correlation coefficients for pairs of elements in different ore types at the Zarshuran deposit

Element pair	Ore type				
	Siliceous	Arsenical	Normal	Pyritic	Carbonaceous
Au to As	0.83	0.48	0.31	0.99	0.79
Au to Sb	0.47	−0.23	−0.06	0.98	−0.10
As to Sb	0.31	0.13	0.69	0.99	0.52

with realgar (AsS), lorandite ($TlAsS_2$) and simonite ($TlHgAs_3S_6$) in orpiment-dominated arsenical ore formed during late stage mineralisation (Mehrabi 1997). There is a tendency for gold to combine with tellurium in some deposits (Radtke 1985) and hence the small amounts of tellurium in some ores (i.e. samples 57847 and T9-50W) may be associated with gold.

The average concentration of thallium in the samples containing detectable amounts (>2 ppm) of Tl is 27 ppm (very high values have been ignored as unreliable). The very high thallium values in a few samples (e.g. 57847) reflects the presence of lorandite ($TlAsS_2$), galkhaite [$(Hg,Cu,Zn,Tl,Fe)_6(Cs,Tl)(As,Sb)_4S_{12}$] and simonite ($TlHgAs_3S_6$) (Mehrabi 1997).

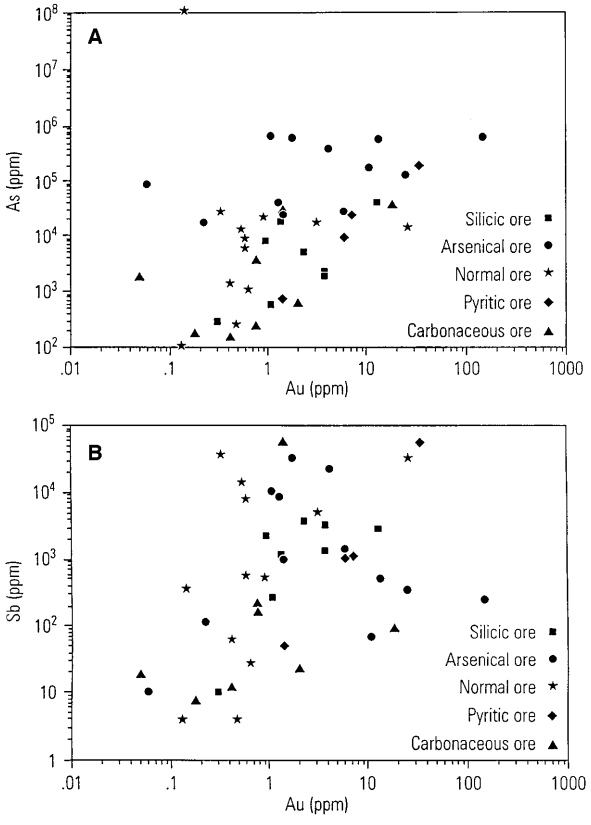

Fig. 4A, B Relationships between gold concentration and **A** arsenic, and **B** antimony for the various ore types at the Zarshuran mine. Note the *different scales*

Paragenetic relations

Several characteristics of the Zarshuran gold deposit make it difficult to deduce the paragenetic sequence. The fine grained nature of gold and associated minerals, the lack of obvious through-going and cross cutting veinlets and the restriction of many veinlets to either hanging wall or foot wall, inhibit conventional paragenetic interpretation. Furthermore the sedimentary host rocks have undergone diagenesis and multiple stages of alteration including weathering, and some of these events are not related to gold mineralisation.

Bariand et al. (1965) discussed the paragenesis of the Zarshuran arsenic mine for the first time and reconstructed the time relationships between pyrite, quartz, stibnite, getchellite and orpiment. For this study veinlets have been used in order to reconstruct a more sophisticated paragenetic sequence of mineralisation at the Zarshuran.

Veins and veinlets

Major through-going veins are sparse, but small discontinuous veinlets, typically 0.5–5 mm in thickness, are common in many localities and yield cross-cutting relationships. Quartz veins are the most abundant type and occur within jasperoids and other silicified rocks. Quartz veins to microveinlets are grey or colourless and the thicker veins contain minor amounts of disseminated pyrite, stibnite and arsenic sulphides. In jasperoids, multiple veining (<2 mm) has produced the microstockwork and boxwork texture.

In detailed microscopic studies, several types of veinlets have been identified in different ore types (Table 5). The cross-cutting relationship of these veinlets is complex and it is difficult to establish a paragenetic sequence of mineralisation based only on cross-cutting. The following summary categorises veinlets and veins on the basis of mineralogy, but also separates veins of the same mineralogy but clearly different ages.

Quartz veinlets formed during all stages of mineralisation. Veinlets (A), formed during the early stage of mineralisation, are nearly pure microcrystalline quartz with no associated sulphide minerals apart from rare minor pyrite. Early minor barite and base metal veinlets (B) cut the early quartz veinlets in jasperoids, and contain up to 0.2 mm subhedral to euhedral barite, pyrite, sphalerite and rarely small inclusions of 10–20 μm size galena in pyrite and sphalerite.

Quartz and pyrite veinlets (C) formed during the main stage of mineralisation and contain disseminated pyrite and arsenian pyrite, mainly with a subhedral to anhedral shape. The sulphides form up to 10% of the veinlets. Veinlets (C), are cut by later stage quartz veinlets (D), of nearly pure microcrystalline quartz, having no preferred orientation, and giving rise to stockwork texture.

Table 5 Characteristics of the main vein and veinlet types in Zarshuran deposit

Veinlet filling	Colour and habit	Grain size	Veinlet width	Veinlet form
Quartz (A)	Grey	Microcrystalline	0.05–0.5 mm	Irregular and discontinuous
Barite-base metal (B)	White grey	Microcrystalline	0.05–0.15 mm	Irregular, moderately discontinuous and cuts early quartz
Quartz + pyrite (C)	Grey	10–30 μm	0.05–2.00 mm	Irregular, moderately continuous
Quartz (D)	White grey	Microcrystalline	0.05–0.1 mm	Stockwork, Irregular, discontinuous
Fluorite ± quartz ± orpiment ± sphalerite (E)	Purple, green and colourless, crystalline	0.1–15 cm	2 mm–5 cm	Irregular, discontinuous and fragmented
Calcite veinlets (F)	White colour, interlocking crystals	1–5 mm	0.1–10 mm	Irregular to planar, moderately continuous, fill vugs
Quartz + orpiment (G)	Yellow colour and crystalline	1–5 mm	2–10 cm	Irregular, discontinuous, open space filling with vuggy texture
Barite (H)	White with interlocking texture	0.1–10 mm	1–10 cm	Irregular and moderately continuous
Calcite vein (I)	White to grey, crystalline and interlocking	0.2–3 cm	120 cm	Planar and moderately regular

Fluorite ± quartz ± orpiment ± sphalerite veins and veinlets (E) formed from the end of the main stage up to late stage of mineralisation. In borehole 9 there is a veining zone of type E veins and veinlets up to 5 m thick. They are normally hosted by carbonaceous and normal ores. Fluorite (purple, green and colourless), is the predominant mineral, with crystals up to 1.5 cm in size, exhibiting oscillatory colour zonation. Quartz and orpiment crystals up to 0.5 cm and zoned crystals of sphalerite up to 0.4 cm also occur. Antimony and antimony-lead sulphides are present as accessory minerals. The earlier type E veins contain only fluorite, with quartz, orpiment and sphalerite observed in the later veins.

Calcite veinlets (F) contain mainly white calcite with open space-filling textures up to 0.5 cm across. Quartz and orpiment veins and veinlets (G) contain euhedral crystals of quartz and orpiment, also with open space-filling textures. Orpiment sometimes contains euhedral inclusions of pyrite up to 40 μm in size. The quartz-orpiment ratio varies in these veins.

Veins (H), formed during the late stage of mineralisation, are the most abundant set of barite veins and are composed of coarse (<1 cm) interlocking crystals. Calcite veins (I), composed of nearly pure coarse calcite, up to 3 cm in width, were emplaced at the late stage mineralisation.

Paragenetic sequence

Because of the presence of several ore and alteration types, and the different mineralogies involved, the paragenetic sequence of each type of ore was studied separately. By considering timing and relations between them, the sequence of hydrothermal activity was established. It is difficult to sort out separate events at a given locality into a definitive time sequence and even more difficult to correlate events between different localities in the ore deposit, because so many of the alteration processes were intermittent and overlapping. Therefore, it is only possible to establish an overall paragenetic sequence, and this is summarised in Fig. 5. The main features are now described.

The *early stage* of hydrothermal activity at Zarshuran is dominated by removal of calcite and precipitation of lesser volumes quartz which resulted in porous jasperoids with small inclusions of calcite remaining. Gold is associated with pyrite and arsenian pyrite in the early jasperoid, but otherwise there is little mineralisation.

The *main stage* of hydrothermal activity is characterised by potassic-argillic alteration, although silification continued. Sulphide minerals become more abundant and even quartz veinlets formed in this stage contain up to 10% pyrite. During this stage, there is minor development of barite and base metal minerals (sphalerite, galena and geochronite) in massive silicified rocks. Petrographic and ore microscopic data suggest that most quartz, clay minerals, hydrothermal pyrite and associated arsenic, antimony, mercury and thallium minerals, were produced during this main stage.

During the *late stage* of hydrothermal activity, arsenic and then base metal sulphides became dominant. The degree of silicification diminished, and veining and open space filling become more common. Veins dominated by barite, quartz, calcite, or fluorite

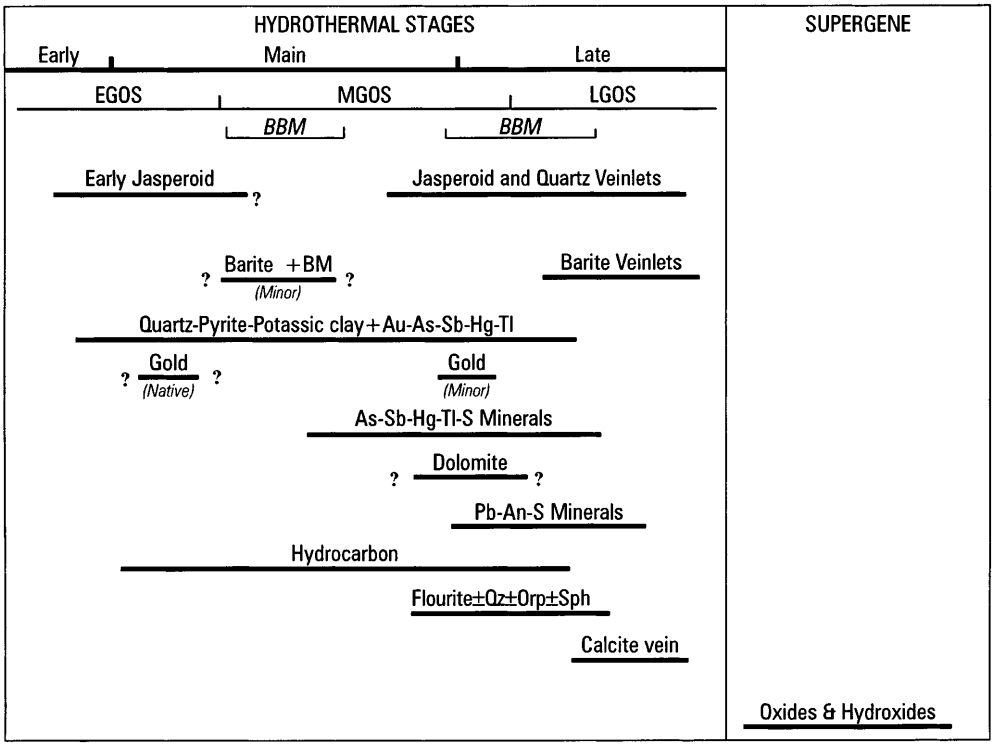

Fig. 5 Overall paragenetic sequence in the Zarshuran gold deposit. Abbreviations; *EGOS*, early gold ore stage; *MGOS*, main gold ore stage; *LGOS*, late gold ore stage; *BBM*, barite and base metal; *Qz*, quartz; *Orp*, orpiment and *Sph*, sphalerite

(±quartz ± orpiment ± sphalerite) formed at this stage, and strong carbonaceous alteration occurred. These features represent a continuum of the hydrothermal processes. Commercial arsenic ore began to form late in the main stage but mainly formed during the late stage of hydrothermal activity. Gold was deposited during both main and late stages of hydrothermal mineralisation.

Fluid inclusions and the physical environment of ore deposition

A range of fluid inclusion types are present in hydrothermal quartz, fluorite, sphalerite, barite and calcite from both veins and host rock, and provide an opportunity to constrain the *P-T* conditions of ore formation. Fluid inclusions have been classified based on their appearance at 20 °C into three main types and nine subtypes (Table 6). Fluids from the different stages of the paragenetic framework were characterised by microthermometry.

The quartz grains of the sedimentary host rock contain inherited primary inclusions with high salinity which are readily distinguished from later fluids. The early stage of mineralisation is associated with very small, two-phase water inclusions. The main stage fluids are characterised by the occurrence of CO_2 fluids, with low salinity water. The water-bearing fluids have relatively high homogenisation temperatures. Towards the late stage, CH_4 appears in inclusions, probably reflecting organic matter maturation. CH_4 ± CO_2, pure CO_2 and multiple generations of aqueous inclusions of varied salinity and homogenisation temperature are all present in samples related to the late stage of mineralisation. A summary of the fluid inclusion data is presented in Table 7.

The intersection of isochores from coexisting CH_4, CO_2 and H_2O inclusions (data from Table 7), together with geological evidence, has been used to calculate the P_f-T conditions of entrapment (Fig. 6). These are: 216 ± 32 °C at 865 ± 375 bar during the early stage, 264 ± 38 °C at 1150 ± 150 bar during the main stage and 185 ± 40 °C to 220 ± 35 °C at 865 ± 375 to 1175 ± 225 bar during the late stage of mineralisation (Fig. 6).

The estimated temperatures and pressures indicate that the Zarshuran deposit formed at a higher pressure than classic epithermal deposits. Typical lithostatic and hydrostatic gradients of 250 and 80 bar/km require depths of at least 3.8 ± 1.8 km and 11.8 ± 5.7 km respectively to reach the estimated pressure. A pure lithostatic gradient in P_f is unlikely because this would imply very low permeabilities, but the estimated depth based on hydrostatic conditions seems to geologically unreasonable. Hence vertical fluid pressure gradients appreciably in excess of normal hydrostatic are required to accommodate hydrothermal mineralisation at the depth of a few kilometres, required by geological considerations. Alternation of a hydrostatic fluid environment with near-lithostatic (overpressured) conditions could however account for both the fluid pressure and the abundant evidence for flow. We conclude that it is likely that pressure fluctuated, but was frequently close to lithostatic when inclusions were trapped.

Table 6 Room temperature characteristics of the major types of fluid inclusions in present in samples formed at different stage of mineralisation at the Zarshuran deposit

Group	Major contents	Comment	Origin	Description	Stage
1A	One phase $CH_4 \pm CO_2$	Nucleate bubble below −82.4 °C	P or PS	Equant, high relief and dark appearance	LS
1B	One phase CO_2	Triple point melting near −56.6 °C	P or PS	Equant, some with dark appearance	MS-LS
1C	One phase H_2O	Sometimes nucleate bubble during cooling	PS and S	Equant and empty looking	LS
2A	Two phase H_2O	Very saline	P	Subhedral to equant	SD-LS
2B	Two phase H_2O with trace of CO_2	Dark halo around the bubbles	PS and P	Negative xtal (P) and equant (PS)	LS
2C	Two phase H_2O	Normal aqueous inclusions	S-PS-P	Equant, subhedral and negative xtal equant and clear	ES-MS-LS-BBM
2D	Two phase H_2O	Very low salinity, $Tm < -3$	S-PS		LS
3A	Three phase H_2O-$CO_2 \pm CH_4 \pm N_2$	CO_2 homogenised to liquid, $Th > 280$ °C	P	Small size (5 μm)	MS
3B	Three phase CO_2 rich with minor $H_2O \pm CH_4$	Homogenised to liquid CO_2	P	Big bubble and equant shape	MS

Abbreviations: P, primary; PS, psudosecondary; S, secondary; ES, early stage; MS, main stage; LS, late stage; BBM, barite and base metal and SD, sedimentary

Geochronology

In three other prospects in the Zarshuran area, polymetallic mineralisation occurred in the Tertiary, which coincides with Miocene volcanic activity in the area (Mohajer et al. 1989). In the Zarshuran deposit, mineralisation is hosted by a probable Precambrian sequence (Samimi 1992), but the exact ages of the mineralisation and the host rocks are uncertain.

The mineralisation at the Zarshuran occurs in black shale of Zarshuran Unit, whose age is not known with confidence. Miocene volcanic activity in the area has not previously been dated by radiogenic methods.

Methods

The main host rock is the Zarshuran Black Shale Unit which contains ubiquitous illite and sericite. Because mineralisation occurred at relatively low temperatures, clay petrology was coupled with K/Ar dating of clay minerals.

Dating of the sediment-hosted disseminated gold mineralisation at the Zarshuran is difficult because the paragenesis of the submicron gold is difficult to ascertain, and mineralised veins lack dateable minerals or well-defined cross-cutting relations with other datable features. This leaves the dating of hydrothermal illite as the most reliable technique for dating the potassic alteration, and by inference, the mineralisation.

Probable middle Miocene volcanic rocks cover a large area north of Takab. In the mining area, Miocene Volcanics overly Upper Red Formation (Mehrabi 1997). Acid volcanic rocks have been dated by the K/Ar method and andesitic rocks with the Ar/Ar method, following procedures outlined in Rex (1994) and Rex et al. (1993).

Analysed material

Several samples from the Zarshuran Unit were dated, ranging from unmineralised host rock, through weakly mineralised, to highly altered and mineralised rock (Table 8). Samples were characterised by conventional mineralogical methods and some were analysed for gold and total organic carbon. Based on mineralogical data, separate clay-size fractions or whole rock were dated by the K/Ar method.

The samples (Table 8) can be divided into two groups representing the two main original rock types in the Zarshuran Unit; (a) calcareous shale and (b) silty limestone. The argillic alteration of calcareous shale has resulted in more complex alteration mineralogy than in silty limestone. Illite-sericite textures in argillised limestone from the Zarshuran Unit indicate a predominantly hydrothermal origin, making them particularly well suited for dating. These textures include; illite flakes formed in small unoriented fractures (Fig. 7A), formed in secondary porosity around calcite grains, formed by decalcification in association with As-Sb-Fe sulphides (Fig. 7B), illite-sericite matrix associated with skeletal pyrite (Fig. 7C) and intergrown with arsenic sulphides (Fig. 7D).

Hydrothermally altered shale from the Zarshuran Unit has overall the same mineral assemblage as altered silty limestone (illite-sericie + kaolinite + quartz + pyrite) but the argillic alteration product is fine grained and occurs both concentrated along small fractures and in the host rock matrix.

Table 7 Summary of fluid inclusion data from the Zarshuran deposit. The data are presented as minimum, maximum and mean values on successive rows

Stage	Origin	Type	Group*	Sample number	Mineral	Tm_{CO_2} (°C)	Tm (°C)	Td_{cla} (°C)	Th_{CO_2} (°C)	Th_{CH_4} (°C)	Th (°C)
PM	P	Lw	2A	56932	Quartz		−13.5				216.0
							−22.3				140.8
							−15.8				158.5
PM	P	Lw	2A	57524	Quartz		−17.6				214.0
							−20.6				191.0
							−18.9				202.1
ES	S	Lw	2C	57524	Quartz		−4.3				236.3
							−5.3				198.7
							−4.8				216.4
ES	P	Lw	2C	56932	Quartz		−3.2				188.0
							−6.2				145.0
							−4.5				169.2
BBM	P	Lw	2C	56932	Sphalerite		−13.2				212.0
							−13.7				134.0
							−13.5				168.0
MS	P	Lw	2C	57523	Quartz		−4.1				246.0
							−5.1				169.1
							−4.9				216.0
MS	P	Lcw	3A	57523	Quartz	−57.2		9.0	25.6		319.7
			3B			−61.6		5.5	14.2		235.0
						−58.6		7.4	18.6		285.6
MS	P	Lc	1B	57523	Quartz	−59.6			21.1		
						−59.8			20.9		
						−59.7			21.0		
LS	P	Lw	2B	56926	Quartz		−4.4				162.0
							−6.8				149.0
							−5.2				156.4
LS	P	Lw	2C	57521	Fluorite		−7.8				225.0
							−9.6				155.4
							−8.5				213.7
LS	PS	Lw	2B	57521	Fluorite		−4.2				244.5
							−5.5				189.3
							−5.0				229.4
LS	PS	Lw	2C	57521	Fluorite		−3.4				203.4
							−5.9				135.0
											158.2
LS	PS	Lw	2C	57521	Orpiment		−3.6				233.0
							−6.3				143.5
							−4.5				167.1
LS	PS	Lc	1B	57521	Fluorite	−56.7			14.2		
						−57.7			12.0		
						−57.2			12.9		
LS	P	Lw	2A	57525	Fluorite		−18.6				197.3
							−24.8				119.7
							−22.8				145.2
LS	PS	Lw	2B	57525	Fluorite		−8.5				239.0
							−10.9				190.0
							−10.4				212.5
LS	PS	Lw	2C	57525	Fluorite		−8.1				191.1
							−12.3				161.0
							−10.2				178.3
LS	S	Lw	2B	57525	Fluorite		−4.0				196.8
							−5.1				182.0
							−4.4				189.2
LS	S	Lw	2C	57525	Fluorite		−3.8				178.0
							−6.6				126.2
							−4.8				154.8
LS	S	Lw	2D	57525	Fluorite		−1.2				141.9
							−1.6				137.4
							−1.4				139.6
LS	P	Lw	2C	57528	Fluorite		−7.9				154.6
							−8.2				128.1
							−8.0				141.8
LS	PS	Lw	2C	57528	Fluorite		−3.8				170.2
							−5.5				124.4
							−4.8				142.8

Table 7 (Contd.)

Stage	Origin	Type	Group*	Sample number	Mineral	Tm_{CO_2} (°C)	Tm (°C)	Td_{cla} (°C)	Th_{CO_2} (°C)	Th_{CH_4} (°C)	Th (°C)
	PS	Lw	2D	57525	Fluorite		−0.2				142.0
LS							−2.8				128.2
							−1.2				132.5
LS	PS	Lc	1A	57528	Fluorite					−82.9	
										−94.0	
										−87.2	
LS	PS	Lc	1B	57528	Fluorite	−57.1			13.5		
						−58.5			9.0		
						−57.6			11.0		

PM: pre-mineralisation; ES: early stage; MS: main stage and LS: late stage

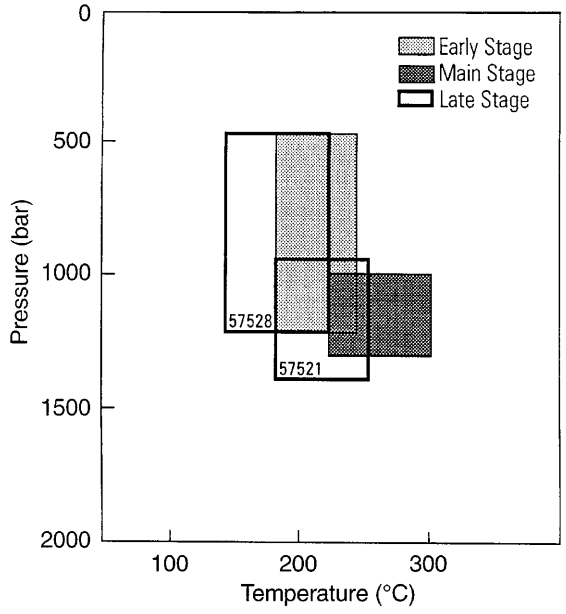

Fig. 6 P-T conditions during different stages of mineralisation at the Zarshuran, based on intersecting isochores

The Miocene volcanic sequence starts with andesitic lavas and passes up into rhyolite and rhyolitic tuff. Twelve samples of volcanic rocks (Table 9) were dated by K/Ar and Ar/Ar methods. The acid volcanic rocks, both whole rock and mineral separates, were dated by K/Ar. Fine grained alteration of andesitic rocks prevented separation of suitable minerals, and therefore whole rocks were dated by the Ar/Ar method.

K/Ar ages of host rock and mineralisation

The K/Ar dates and related chemical data for host rock and argillically altered rocks are shown in Table 10. The interpretation of many of the illite-sericite with respect to the timing of mineralisation is problematic because the samples may contain some older inherited material. The ages obtained from the less than 2 μm size fraction (Table 10) are older than the whole rock ages, indicating that the smaller size fraction contains the older sericite component.

Two samples which represent the host rock (BH9-80.6, unmineralised, and BH2N, weakly mineralised)

Table 8 Location and description of dated samples from the Zarshuran Unit

Sample number	Location	Rock/ore type	Mineralogy	Methods[a]
BH2N	Outcrop of Zarshuran Unit next to BH2	Slightly weathered black shale	Quartz, calcite, sericite, dolomite and pyrite	A-B-E
BH9-80.6	80.6 m depth, BH9	Fresh unmineralised host rock	Calcite, quartz, clay minerals, organic material and pyrite	A-D-E
T8DL68	Exploratory side branch 68 m into tunnel 8 on the left hand side	Black silicified rock	Quartz, sericite, orpiment, realgar, stibnite, sphalerite and galena	A-B-C-E
T8DP	Waste of arsenic mining in tunnel 8	Black colour silicified rock	Quartz, orpiment, sericite, reaglar and pyrite	A-B-C-E
56936	45 m into tunnel 8	Black silicified rock (ES-BBM)	Quartz, orpiment, sericite, pyrite and sphalerite	A-B-C-D-F
57535	216 m depth, BH8	Carbonaceous ore	Quartz, dolomite, clay minerals, organic materials and As-Fe-Zn sulphides	A-B-C-D-E
57548	68.9 m depth, tunnel 8	Altered calcareous shale (MS)	Quartz, orpiment, sericite and pyrite	A-C

[a] Methods used for identification: A: optical microscopy; B: XRD; C: SEM; D: wet chemical analysis (Au-As-Ag-Sb-Te-Tl) and E: total organic carbon analysis. Abbreviations: ES, early stage of mineralisation and BBM, barite and base metal stage

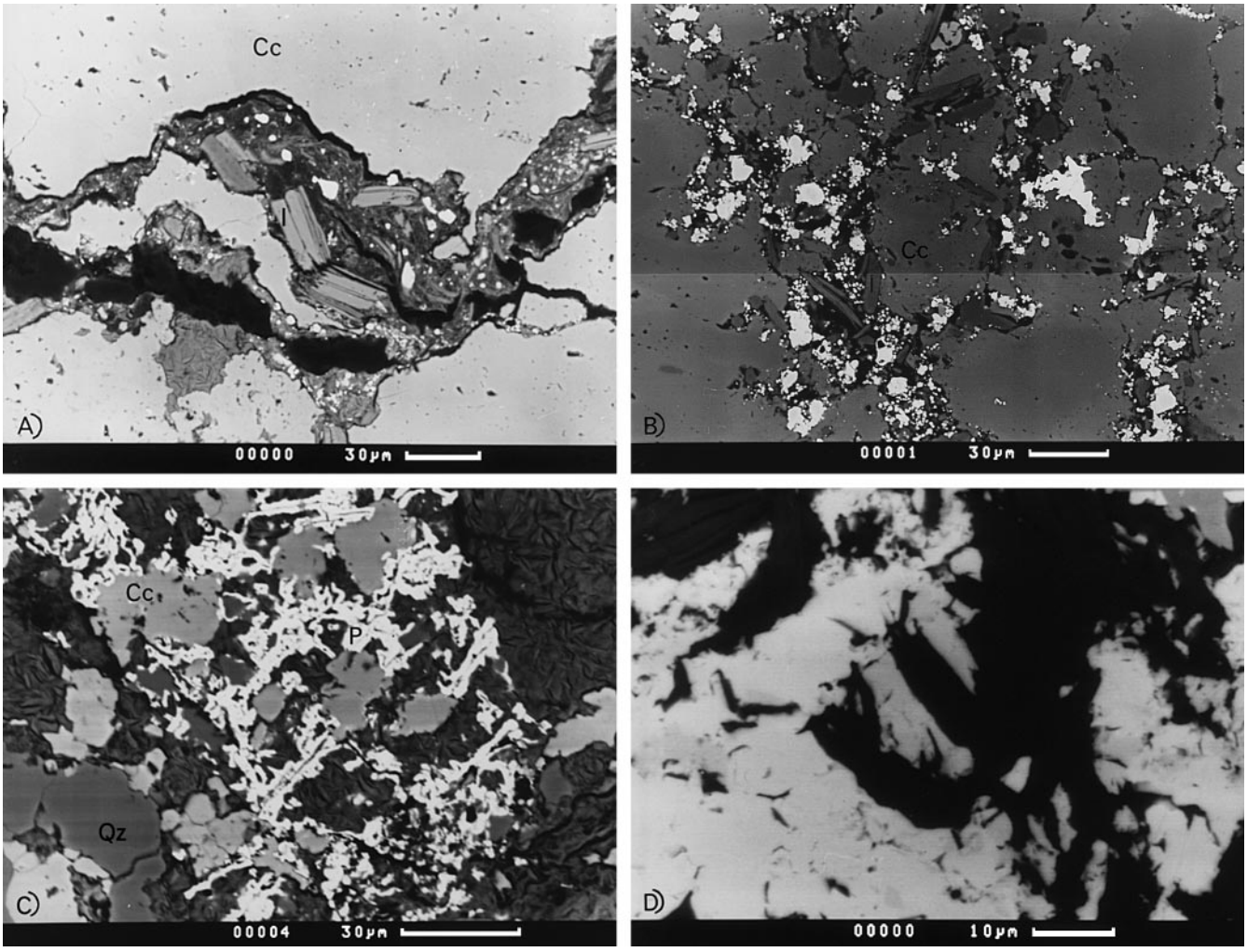

Fig. 7A–D SEM backscattered electron image of hydrothermal alteration textures in limestone layers from the Zarshuran Unit at the Zarshuran deposit. **A** Fracture in limestone filled with fine mixed clays (*dark grey*) pyrite white and coarser flakes of illite-sericite; **B** fine grained limestone with sulphides (*white*) and illite-sericite flakes (*dark grey*) infilling secondary porosity; **C** extensively altered limestone with radiating microlites of illite-sericite (*dark grey*) hosting skeletal pyrite (*white*) and **D** realgar (*white*) with flake of illite-sericite (*grey*) from a veinlet in altered limestone, the two mineral are closely intergrown but realgar locally replacing the phylosilicates. Abbreviations: *C*, calcite; *I*, illite-sericite; *Py*, pyrite, *Qz*, quartz

yield ages of 17.5 ± 0.5 and 24.4 ± 0.7 Ma (Table 10). These ages apparently imply a Miocene age for the Zarshuran Unit, but this may simply reflect resetting of older micas by thermal events during the Miocene.

Ages for argillic alteration, and hence mineralisation, range from 14.2 ± 0.4 to 26.1 ± 0.8 Ma (Table 10). Petrographic evidence indicates that hydrothermal illite-sericite is the predominant K-bearing mineral in samples 57535 and 57548 whereas other samples may contain some older mica. These two samples yield the youngest

Table 9 Location and description of dated Miocene volcanic rocks

Sample number	Location	Rock type
57499	2.5 km north of Zarshuran village	Trachyandesite
57501	Outcrop of volcanic rocks east of Zarshuran village	Porphyritic andesite
57502	Kalakli mountain	Rhyolitic tuff
57504	Chaldagh mountain near old trench	Trachyandesite
57505	Kalakli mountain	Rhyolitic tuff
57507	Kalkli mountain	Rhyolitic tuff
57508	3 km north of Zarshuran village	Porphyritic andesite
57514	1 km north of Zarshuran village	Quartz latite
57515	Chaldagh mountain near old trenches	Trachyandesite
57516	Chaldagh mountain near old trenches	Rhyolitic tuff
57852	300 m north of mine office in Zarshuran village	Porphyritic andesite
57855	500 m north of mine office in Zarshuran village	Porphyritic andesite

Table 10 K/Ar ages of host rock and argillic alteration at the Zarshuran deposit

Sample number	Mineral	K (%)	Vol^{40} Ar$_{(Rad.)}$ Scc/g $\times 10^{-5}$	^{40}Ar$_{(Rad.)}$ (%)	Age (Ma)
BH2N	Sp	4.752	0.4543	81.5	24.4 ± 0.7
BH9-80.6	WR	2.632	0.1796	72.2	17.5 ± 0.5
T8DL68	Sp	4.307	0.4053	58.7	24.0 ± 0.7
T8DP	Sp	2.054	0.2102	43.6	26.1 ± 0.8
56936	Sp	1.729	0.1468	42.6	21.7 ± 0.9
57535	WR	2.239	0.1244	55.4	14.2 ± 0.4
57548	WR	0.743	0.0414	20.8	14.3 ± 0.4

Sp: separated clay size fraction; WR: whole rock

ages (about 14.3 Ma) and thus this is the preferred age for the mineralisation. Samples 56936, T8DL68 and T8DP are mineralised black shales, and therefore the presence of older illite-sericite from the original rocks may have affected the result. In addition the difference between ages of separated clay size fraction and whole rock suggest the possibility of a mixed age for these samples.

K/Ar and Ar/Ar ages of volcanic rocks

The Ar/Ar ages of andesitic rocks from the base of the volcanic sequence are 14.4 ± 0.3 to 16.2 + 0.3 Ma (Table 11 and Fig. 8). Ages of the overlying acidic volcanic rocks range from 11.1 ± 0.3 to 13 ± 0.4 Ma (Table 12) except for sample 57502 (15.7 ± 0.5 Ma) which may have experienced K-loss, because the potassium concentration in this sample is less than expected from separated illite-sericite (compare with samples 57505 and 57507). These ages of 16.2 to 11.1 Ma are in good agreement with stratigraphic evidence.

Discussion

The Miocene ages obtained for the host rocks of 17.5 ± 0.5 and 24.4 ± 0.7 Ma contradict stratigraphic evidence for a late Precambrian age (Samimi 1992) but may have been partially reset despite the absence of mineralisation.

In contrast to the clay size fraction dates, which are older than the dates obtained for the volcanic activity (11.1 ± 0.3 to 16.4 ± 0.3), the ages of argillic alteration in limestone (sample 57535) and of intense argillic alteration in shale (sample 57548) are in the volcanic age bracket. The argillic alteration in the limestone sample represents new growth without an inherited component, and should therefore provide the best indication of the age of hydrothermal gold mineralisation at the Zarshuran deposit, i.e. 14.3 ± 0.4 Ma.

These results (Fig. 9) demonstrate that mineralisation was contemporaneous with the early Miocene volcanism at Zarshuran. Further significance of this conclusion is that in the type district for Carlin-style mineralisation it has proved difficult to demonstrate such as relationship and hence the role of magmatism in the ore genesis has been controversial (Bagby and Berger 1985; Thorman and Christensen 1991).

The classification and origin of the Zarshuran mineralisation

The characteristic features of mineralisation at Zarshuran are: (a) submicron to micron size disseminated gold, (b) calcareous and carbonaceous shale and limestone host rocks, (c) presence of the elements As, Sb, Hg and Tl associated with the gold, and (d) associated decalcification, silicification and argillisation of wall rocks. These features are similar to those of the sediment-hosted gold deposits of the "Carlin-type", in western North America.

A large amount of research has been done on Carlin-type deposits, also known as "sediment-hosted disseminated precious-metal deposits" (e.g. Bagby and Berger 1985), "sediment-hosted gold deposits" (e.g. Sillitoe and Bonham 1990) and including some "epithermal replacement deposits" (e.g. White and Hedinquist 1990). Their major characteristics have been described in detail in number of publications (Radtke and Dickson 1976; Bagby and Berger 1985; Percival et al. 1988, Berger and Henley 1989; Berger and Bagby 1991). Although they display considerable variation in their geologic characteristics, there are number of similarities that provide cohesiveness and definition to the deposit type.

The key physical and chemical features of mineralisation at the Zarshuran, are compared with those of the Carlin and Getchell deposits of western North America in Table 13. The Zarshuran and Great Basin deposits occur in host rocks of similar lithology, and both contain very fine-grained gold associated with As, Sb, Hg and Tl. Likewise, the same types of hydrothermal alteration are present in both. The similarities between the physical and chemical features of mineralisation at the Zarshuran and in Carlin-type deposits suggest strongly that the Zarshuran deposit is an example of Carlin-type mineralisation.

Early workers inferred a shallow environment for the genesis of Carlin-type gold deposits because: (a) the suite of trace elements (As, Sb, Au, Hg, Tl) is also reported in many epithermal and hot spring deposits, (b) vuggy and open space filling textures occur and a maximum burial depth of 300 m was inferred from geological information for Getchell (Joralemon 1951, 1975), and (c) a maximum depth of 300–500 m was inferred for the Carlin deposit based on evidence for boiling, inferred from fluid inclusions (Radtke et al. 1980; Radtke 1985).

In contrast, recent research suggests that the environment of deposition is probably deeper (i.e. >500 m). Roberts (1986) estimated at least 520–910 m of cover above the Carlin ore zone during ore formation. Deep ore has been discovered in Post-Betz (Bettles 1989), near

Table 11 K/Ar ages of Miocene volcanic rocks

Temperature (°C)	Volume (10^{-9} cm^3 STP)			Ca/K	*40/$^{39}Ar_K$	^{40}Ar (%Atm.)	Age (Ma)	Error (Ma)	$^{39}Ar_K$ (%)
	$^{39}Ar_K$	$^{37}Ar_{Ca}$	$^{38}Ar_{Cl}$						
Sample: 57501 (whole rock), run 2182, sample weight 0.05999 g, J value = 0.00521 ± 1.0%									
650	6.2	2.1	0.42	0.69	1.666	77.5	15.6	1.2	12.3
730	10.7	10.9	0.22	2.02	1.780	51.3	16.7	0.3	21.4
800	8.4	3.9	0.18	0.93	1.827	7.1	17.1	0.3	16.7
915	6.1	3.4	0.19	1.12	1.684	22.2	15.8	0.6	12.1
1005	10.6	4.5	0.52	0.86	1.744	28.5	16.3	0.4	21.0
1100	5.7	4.4	0.37	1.54	1.585	36.8	14.8	0.5	11.4
1300	2.6	4.6	0.26	3.58	2.212	42.4	20.7	1.5	5.1
Age derived from step 1–6: 16.2 ± 0.3 Ma K = 2.3 wt.%, $^{40}Ar = 14.7 \times 10^{-7}$ cm^3 g^{-1}									
Sample: 57508 (whole rock), run 2183, sample weight 0.06341 g, J value = 0.00521 ± 1.0%									
720	10.8	3.7	0.52	0.70	1.463	81.0	13.7	0.4	22.0
800	6.3	4.1	0.21	1.30	1.750	31.2	16.4	0.7	12.7
895	7.2	4.5	0.30	1.20	1.795	24.4	16.8	0.2	14.6
1000	12.8	6.8	0.62	1.10	1.664	28.9	15.6	0.2	25.8
1090	5.2	3.3	0.29	1.30	1.603	33.3	15.0	1.2	10.5
1245	5.5	6.4	0.40	2.30	1.722	51.0	16.1	0.5	11.1
1295	1.6	1.6	0.11	2.00	3.119	59.4	29.1	1.7	3.3
Age derived from step 1–6: 15.9 ± 0.3 Ma K = 2.1 wt.%, $^{40}Ar = 13.2 \times 10^{-7}$ cm^3 g^{-1}									
Sample: 57852 (whole rock), run 2184, sample weight 0.06149 g, J value = 0.00525 ± 1.0%									
650	4.5	3.4	0.23	1.51	1.975	92.8	18.6	0.8	8.4
710	4.8	6.8	0.10	2.83	1.710	83.2	16.1	0.6	8.8
800	10.1	4.3	0.16	0.86	1.743	24.1	16.4	0.3	18.5
895	10.0	5.0	0.24	1.00	1.697	31.3	16.0	0.4	18.4
1020	12.3	5.6	0.38	0.91	1.765	44.9	16.6	0.4	22.6
1100	6.1	3.6	0.21	1.17	1.796	54.7	16.9	0.6	11.2
1360	6.6	9.2	0.39	2.79	7.087	23.8	65.9	0.6	12.1
Age derived from step 1–6: 16.4 ± 0.3 Ma K = 2.4 wt.%, $^{40}Ar = 21.3 \times 10^{-7}$ cm^3 g^{-1}									
Sample: 57855 (whole rock), run 2185, sample weight 0.06481 g, J value = 0.00525 ± 1.0%									
665	9.7	2.6	0.50	0.52	1.475	60.6	13.9	0.2	17.2
710	4.0	1.7	0.07	0.84	1.722	9.9	16.2	0.5	7.1
800	4.9	2.2	0.11	0.89	1.446	23.0	13.6	1.0	8.7
905	9.1	2.8	0.27	0.62	1.633	10.4	15.4	0.4	16.1
1000	6.7	2.2	0.27	0.65	1.617	17.4	15.3	0.6	11.8
1100	16.4	7.2	0.77	0.87	1.439	22.8	13.6	0.3	29.0
1300	5.7	4.4	0.43	1.54	1.832	18.2	17.3	0.6	10.1
Age derived from step 1–6: 14.4 ± 0.3 Ma K = 2.4 wt.%, $^{40}Ar = 13.6 \times 10^{-7}$ cm^3 g^{-1}									

Gold Quarry mine (Rota 1987) and in Getchell (Berger 1985). Kuehn and Rose (1995) calculated a depth of 3.8 ± 1.9 km (800 ± 400 bar pressure) for mineralisation at Carlin, while fluid inclusion isochore intersections suggest pressures of 870 ± 220 and 850 ± 300 bar for different stages of mineralisation at Gold Quarry (Sha 1993). These results are similar to those reported here for Zarshuran, based on similar criteria.

Three contrasting genetic models have been suggested for Carlin-type deposits. The first is that they are linked to magmatism, and are probably distal products of magmatic hydrothermal fluids (Radtke et al. 1980; Radtke 1985; Alvarez and Noble 1988; Sillitoe and Bonham 1990; Arehart et al. 1993). The second is that the major fluid components and metals were released during regional metamorphism of supercrustal rocks (Seedorff 1991; Phillips and Powell 1993). The third model is that Carlin-type deposits develop in (meta)sedimentary terranes as a result of regional fluid circulation due to crustal extension, without any link to magmatism or other heating events (Ilchik and Barton 1997).

The Great Basin region experienced igneous and volcanic activity throughout the Tertiary (Joralemon 1951; Radtke 1985; Rota and Hausen 1991), and a number of jasperiod-hosted gold deposits have been indirectly inferred to be mid-Tertiary by Seedorff (1991). Miocene or younger ages were reported by Radtke (1985)

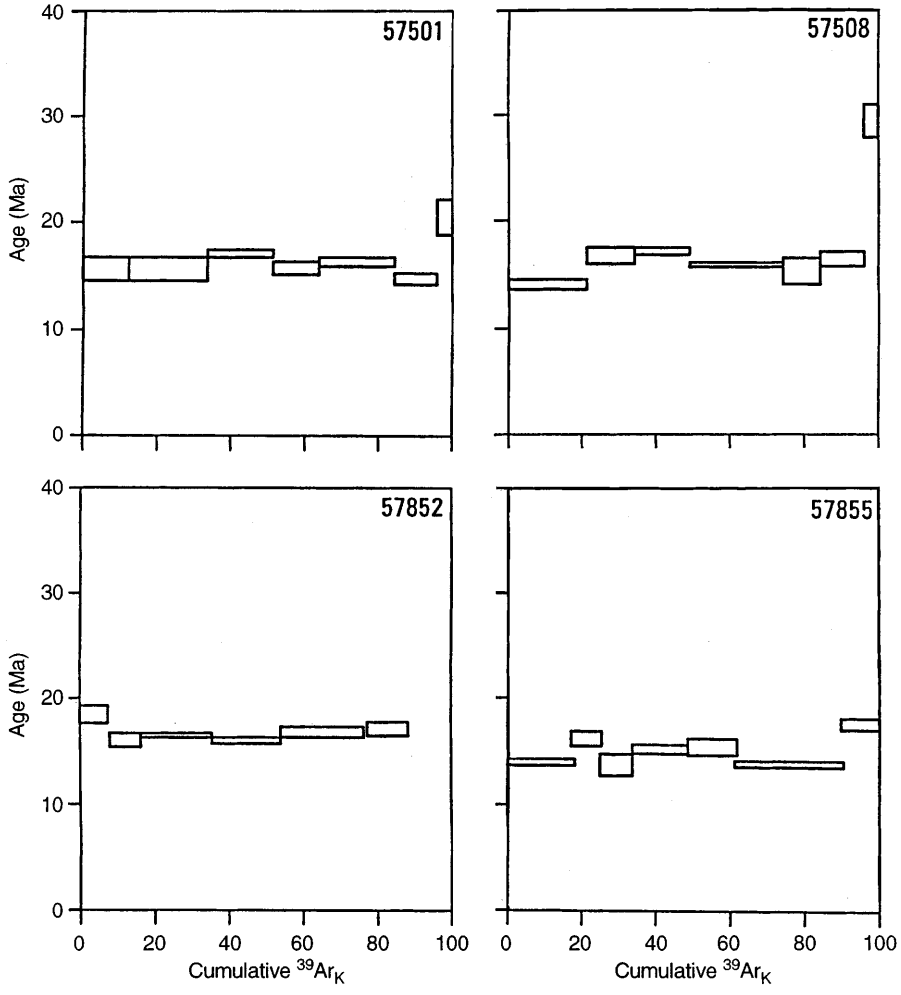

Fig. 8 Age spectra for six step heating and their apparent age (Ma) for andesitic rocks from the base of volcanic sequence

Table 12 Results of Ar/Ar analysis of Miocene volcanic rocks

Sample number	Mineral/whole rock (WR)	K (%)	Vol $^{40}Ar_{(Rad)}$ Scc/g $\times 10^{-5}$	$^{40}Ar_{(Rad)}$ (%)	Age (Ma)
57499	WR	1.98	0.1010	26.4	13.1 ± 0.4
57502	Illite	4.55	0.2785	12.1	15.7 ± 0.5
57504	WR	2.95	0.1405	18.3	12.2 ± 0.4
57505	Illite	6.99	0.3207	17.7	11.8 ± 0.4
57507	Illite	8.28	0.3590	69.1	11.1 ± 0.3
57514	WR	2.38	0.1186	22.9	12.8 ± 0.4
57515	WR	2.22	0.1503	57.6	12.0 ± 0.4
57516	WR	3.45	0.1626	72.9	12.1 ± 0.4

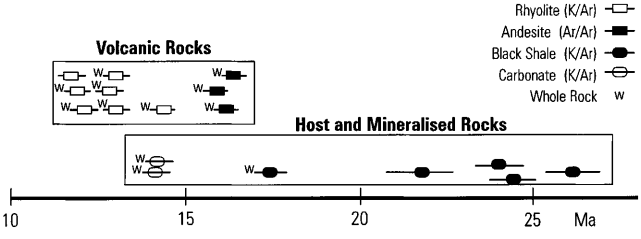

Fig. 9 Compilation of all geochronologic data for volcanic rocks, host and mineralised rocks

for igneous rocks thought to be the possible heat source for Carlin mineralisation; and Tertiary mineralisation ages have been deduced by other workers also. In contrast, a pre-volcanic, Cretaceous age has been suggested by various workers, based on K/Ar dates of alteration minerals thought to be related to gold mineralisation (Silberman and McKee 1971; Silberman et al. 1974; Berger and Taylor 1980; Bonham 1985; Osterberg 1990; Wilson and Parry 1995; Arehart et al. 1993).

Mineralisation at Zarshuran occurred in close spatial and temporal proximity to volcanic activity. This clearly supports a close association between mineralisation and magmatism, as has been inferred for many deposits in the Great Basin region. The age relations appear to be less ambiguous at Zarshuran, and provide clear evidence

Table 13 Comparison of key geological and chemical features of the Zarshuran with those of typical Carlin-type deposits of western North America

	Zarshuran	Carlin[a]	Getchell[b]
Host rock	Precambrian black calcareous silty shale with interbedded limestone	Silurian-Devonian laminated silty to sandy, carbonaceous dolomitic limestone	Cambrian phyllitic shale with interbed limestone
Structural controls	High angle normal fault and cross cutting fault in inlier of Iman Khan double plunged anticline	Steeply dipping faults NW of Tuscarora anticline. Robert Mountains thrust fault	Steeply dipping faults. Isoclinally folded sedimentary rocks
Alteration	Decalcification, silicification argillisation and enrichment in organic carbon	Decalcification, silicification and argillisation, carbon remobilisation and acid leaching	Decalcification, silicification and argillisation
Chemical changes in mineralisation	Introduced: Si, Fe, S, As, Sb, Au, Hg, Tl, F, Ba, Zn, Pb Removed: Ca and Mg	Introduced: Si, Fe, S, Au, As, Hg, Sb, Ba, Tl, Cu, Pb, Zn Removed Ca and Mg	Introduced: Si, Fe, S, Au, As, Sb, Hg, Tl, F, Ba, Te, Se Removed Ca and Mg
Hypogene ore mineralogy	Quartz, pyrite, arsenian, pyrite, orpiment, stibnite, fluorite, barite, cinnabar, sphalerite and galena	Quartz, calcite, pyrite, arsenian, pyrite, realgar, orpiment, stibnite, cinnabar and barite	Quartz, calcite, pyrite, arsenopyrite, marcasite, realgar, orpiment, stibnite, cinnabar, barite, fluorite and chalcopyrite
Associated igneous rocks	Miocene (11.1–16.4 Ma) volcanics mainly andesite	Cretaceous (127 Ma) intermediate composition dikes, altered and mineralised	Cretaceous (90 Ma) granodiorite pluton in the Osgood Mountains associate with intermediate porphyritic dikes

[a] Adkins and Rota (1984); Hausen (1981); Radtke (1985); Bagby and Berger (1985); Berger and Bagby (1991)
[b] Joralemon (1951); Berger and Taylor (1980); Bagby and Berger (1985); Berger and Bagby (1991)

of a temporal as well as spatial link between mineralisation and volcanism.

Models of origin

The purpose of this section is to develop possible genetic models for mineralisation at the Zarshuran based on data from the present study. The constraints on the model of hydrothermal mineralisation at Zarshuran are: (1) formation depth of 3 km or more, (2) restriction of the main ore bodies to black shale, (3) complex paragenesis and lack of zoning in mineralisation and alteration, (4) presence of at least two fluids, (5) presence of wide range of fluid inclusion types, sometimes even in a single sample, (6) presence of high density CO_2- and CH_4- bearing fluids, (7) temporal and spatial association with Miocene magmatic activity, and (8) wide fluctuations in fluid density inferred from fluid inclusions.

Fluid inclusion variability could be interpreted in general terms as the result of boiling, fluid mixing, or fluid-rock interaction.

Boiling is commonly cited to explain increases in salinity, however aqueous vapour inclusions have not been observed at Zarshuran. Furthermore, the inferred pressure of entrapment (945 $\pm$ 445 bar) is outside the two-phase region for H_2O-NaCl-CO_2 fluids at the inferred temperature.

Water-rock interaction is another possible cause for variations in fluid salinity, either through leaching Cl from the rock by adding or removing H_2O from the fluid. Water-rock interaction was important in the hydrothermal system evolution at the Zarshuran, as evidenced by widely distributed wall rock alteration including decalcification, silicification, argillisation and dolomitisation. The presence of illite and kaolinite in the alteration assemblage indicates that the fluid was acidic, but the extensive metasomatism suggests large water rock ratios, whereas salinity changes are likely only in rock-dominated systems.

The preferred explanation for the observed salinity variation is therefore mixing of two or more fluids. The major differences between the early stage fluids and the main and the late stage fluids, as well as the variability at certain stages, indicate that the Zarshuran deposit formed by interaction of at least two fluids. The presence of very low salinity, low temperature fluids and moderate to high salinity fluids trapped at variable temperatures may reflect the end members, for example meteoric and magmatic waters. A 5 m veined zone in bore-hole 8 contains inclusions of low temperature fluid in the upper part, but high temperature fluid in the lower part, with up to 100 °C difference, and is consistent with mixing of cold meteoric water with a hot saline fluid.

The mixing of two fluids in a deep environment has been proposed for Carlin (Kuehn and Rose 1995) and Getchell (Cline et al. 1996) with involvement of a CO_2-rich overpressured fluid (Kuehn and Rose 1995) of either magmatic or metamorphic source, or both. Although Kuehn and Rose (1995) noted that "any direct spatial, temporal or geochemical link to intrusions that might generate a CO_2-rich fluids from magmatic emanations or

skarn formation is at present obscure at Carlin mine'', this is clearly not the case at Zarshuran. The association of the mineralisation with Miocene volcanic activity, the presence of gold, antimony and arsenic mineralisation in quartz veins hosted by Miocene volcanic rocks in the mining area, and the gas-rich fluid inclusions all suggest that magmatic fluid input is important for the Zarshuran hydrothermal mineralisation.

Causes of gold mineralisation

Both pH and fO_2 have opposing effects on gold and arsenic solubilities, and so it is unlikely that Au and As were transported and precipitated together as a result of simple changes in the geochemical environment of an ore fluid. Instead, the association is likely to reflect either kinetic controls on metal precipitation or a complex path of fluid evolution, or both.

There is no direct way to determine the source of gold and volatile metals at Zarshuran. Geochemical modelling (Mehrabi 1997) indicates that an oxidised S, As-rich fluid may have acquired gold as a result of mild reduction by wall rocks, while As remained in solution. There is an average of 384 ppb gold in Precambrian metamorphic rocks of the Iman Khan Unit, (Taddaion 1991). If the Zarshuran shale acted as a seal for an overpressured compartment in the underlying Iman Khan Unit, they may have provided a source of gold.

Figure 10 is a schematic diagram illustrating a possible deep environment for mineralisation at the Zarshuran. The diagram shows a magmatic source for gas-rich, CO_2-bearing fluid with As and S, which mixes with meteoric fluid. A contribution from basin brines trapped prior to pressure seal development is also possible, but a magmatic saline fluid contribution cannot be ruled out. The mixing is inferred to occur at the pressure seal (Zarshuran Unit), separating the overpressured and normally-pressured environments, and mineral precipitation occurs in part because the geochemical barrier (Zarshuran Black shale) provides a strongly reducing environment to trigger As-precipitation. Gold may have coprecipitated for kinetic reasons, or because of massive removal of S from the fluid in arsenic sulphides (Mehrabi 1997 and in preparation).

The most likely locations for leakage from beneath the pressure seal provided by the Zarshuran Black Shale would be faults or the axis of the Iman Khan anticline (see Fig. 3). In this model, the deep, hot, overpressured gas-bearing fluid would ascend along fractures to the site of the ore body at a palaeodepth of about 4.5 km. Episodic break-outs would allow it to mix with hydrostatic-pressured fluid with hydraulic connection to the surface. The main gold ore stage fluids contain mainly CO_2 and minor CH_4, but in the late gold ore stage CH_4 became dominant, which suggests that it was generated after organic material had been maturated. It should be noted that the CO_2, metal and water may have come from separate sources; CO_2 and H_2S from magma, water primarily from the surface, and metals from the magma or from leaching of the Precambrian rock column. We assume that the overpressured fluid is sufficiently slow moving to approach chemical equilibrium with its host for much of the time.

In detail, the episodic nature of the mixing due to break outs from the pressure seal would account for shifts in the locus of deposition, and different flow rates, fluid pressure and fluid chemistry at every break out could change the type of mineral precipitated and the nature of the trapped fluid inclusions in a very complex manner accounting for the complex mineral paragenesis and zoning and the wide range of fluid inclusions within individual samples observed in Zarshuran. In addition to abrupt pressure drop, several chemical processes may occur together in this mixing environment, and can lead to mineral deposition; notably dilution, changes in pH and fO_2, and cooling.

Evolution of ore-deposition processes took place in the following stages, inferred from this study, which are presented schematically in Fig. 10.

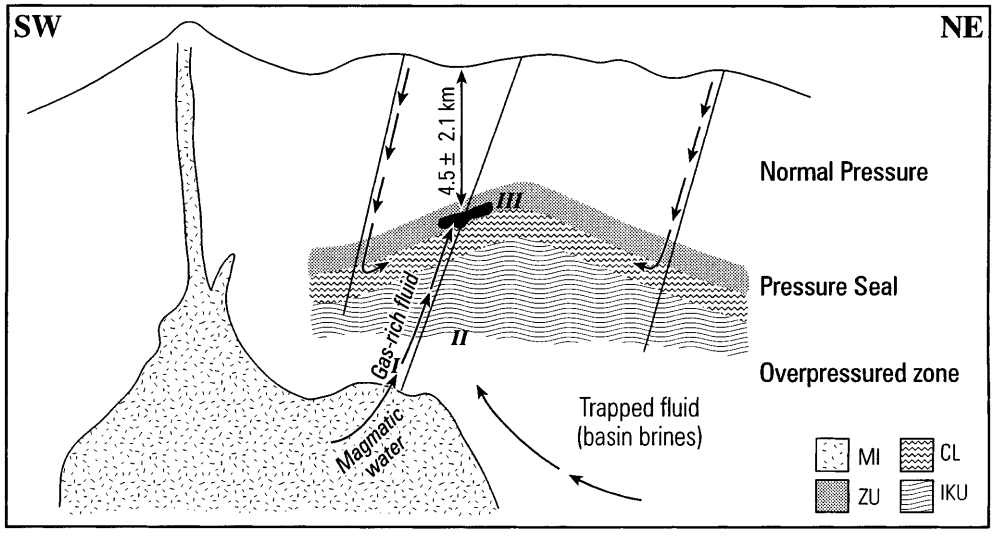

Fig. 10 Schematic model for the development of Zarshuran deposit. *I*, input of magmatic gas-rich fluid; *II*, possible mixing of magmatic fluid with brines in the Precambrian basement, equilibration of fluid with wall rocks may lead to uptake of gold; *III*, break-out through the barrier of the Zarshuran Unit leads to mixing of deeper, hotter fluid with cooler, H_2S-poor meteoric water inside the black shale unit, coupled to redox reactions. The deposit forms at this point. Abbreviations: *MV*, Miocene magmatic rocks; *ZU*, Zarshuran Unit (black shale); *CL*, Chaldagh Limestone, and *IKU*, Iman Khan Unit (greenschist)

a. Magmatic fluids migrate into the uplifting Iman Khan anticline, which is probably sealed with shale, providing an overpressured compartment.

b. Magmatic fluid mixed with trapped fluid (possibly basin brines) in the Precambrian basement rocks, and reacted with them. The initial weakly acidic fluid reacted with carbonate in calcareous black shale and limestone and replaced them with lesser amount of silica (decalcification and silicification), thereby increasing the permeability and porosity of the main host rock and preparing it for further fluid circulation. Probably this is the reason for the presence of barren jasperoid in the early stage of mineralisation.

c. Fluids reach thermal and chemical equilibrium with late Precambrian country rocks inside the overpressured compartment, acquiring gold in solution.

d. There are successive, episodic seal break outs, as a result of which the ore fluid mixes with colder meteoric fluid and reacts with black shale. The changes in P-T with each break out, combined with changes in pH, fO_2 and sulphur concentration in the fluid, resulted in arsenic and gold precipitation.

e. With time, the input of magmatic fluid decreases, and resealing becomes less efficient, leading to deep geothermal circulation and precipitation of quartz, orpiment, calcite and barite with base metal minerals in veins.

Implications for sediment-hosted disseminated gold deposits elsewhere

Many mineralogical and geological features of mineralisation at the Zarshuran are similar to those of sediment-hosted disseminated gold deposits of "Carlin type" in western North America. While many uncertainties remain in our understanding of this class of ore body, the similarities between Zarshuran and other deposits indicates that their formation has been repeated in space and time, and clarifies the type of geological setting in which they develop.

At Zarshuran, the geochronologic data indicates clearly that mineralisation accompanied Miocene volcanism (Fig. 9). This is analogous to the model of mid-Tertiary mineralisation at Carlin. Furthermore the evidence on the depth of mineralisation at Zarshuran, like recent work in Nevada, supports an origin at mesothermal depth. The inferred deep origin for Zarshuran and other disseminated sediment-hosted gold deposits suggests the possibility of additional gold ore occurring below the present working levels and indicates a better preservation potential than for some shallow, epithermal ore bodies.

Acknowledgements For their assistance in the analytical work, we would like to thank: Dave Banks (all aspects of fluid inclusion studies), Eric Condliffe (electron microprobe), Geoff Lloyd (SEM), Dave Rex, Rod Green and Phil Guise (K/Ar and Ar/Ar dating), Simon Bottrell and Dave Hatfield (organic carbon geochemistry), Alan Gray (XRD). We are also grateful to Bob Cliff for his comments on the geochronological interpretation, and to an anonymous referee for a particularly careful and helpful review. BM acknowledges the Iranian Ministry of Culture and Higher Education for a PhD scholarship and thanks the Zarshuran mine staff for providing access and cooperation.

References

Adkins JR, Rota JC (1984) General geology of the Carlin Gold Mine. In: Johnson JL (ed) Field trip guidebook, exploration for ore deposits in the North American Cordillera. Association of Exploration Geochemists pp 17–23

Alavi M, Hajian J, Amidi M, Bolourchi H (1982) Geology of Takab-Saein-Qal'eh. Geol Surv Iran, Rep 50

Alvarez AA, Noble DC (1988) Sedimentary rock-hosted disseminated precious metal mineralization at Purisima Concepcion, Yauricocha district, central Peru. Econ Geol 83: 1368–1378

Arehart GB, Foland KF, Naeser CW, Kesler SE (1993) $^{40}Ar/^{39}Ar$, K/Ar and fission track geochronology of sediment-hosted disseminated gold deposit at Post-Betz, Carlin trend, northeastern Nevada, Econ Geol 88: 622–646

Bagby WC, Berger BR (1985) Geologic characteristics of sediment-hosted disseminated precious metal deposit in the western United States. In: Berger BR, Bethke PM (eds) Geology and geochemistry of epithermal systems. Rev Econ Geol 2: 169–202

Bakken BM, Einaudi MT (1986) Spatial and temporal relation between wall rock alteration and gold mineralization, Main Pit, Carlin gold mine, Nevada, USA, In: MacDonald AJ (ed) Gold '86 Willowdale Ontario Konsult Internat Inc pp 388–403

Bariand P (1962) Contribution a' la mineralogie de l' Iran. PhD thesis, Université de Paris, Faculte des Sciences, Ser A. 980

Bariand P, Cesborn F, Agrinier H, Geffroy J, Issakhanian V (1965) La Getchellite $AsSbS_3$ of Zarehshuran, Afshar, Iran. Bull Soc Fr Mineral Crystalogr 91: 403–406

Barliand P, Pelissier G (1972) Origine de l' ore de Zarehshuran. Bull Soc Fr Mineral Crystalogr 95: 625–629

Berger BR (1985) Geological and geochemical relationships at the Getchell mine and vicinity, Humboldt County, Nevada. In: Hollister VF (ed) Discoveries of epithermal precious metal deposits. Society of Mining Engineers, New York, pp 51–59

Berger BR, Bagby WC (1991) The geology and origin of Carlin-type deposit. In: Foster RP (ed) Gold metallogeny and exploration. Blackie, Glasgow, pp 210–248

Berger BR, Henley RW (1989) Advances in the understanding of epithermal gold-silver deposits-With special references to deposits of the western United States. In: Keays R, Ramsy R, Groves D (eds) The geology of gold deposits: the prospective in 1988. Econ Geol Monogr 6: 405–423

Berger BR, Taylor BE (1980) Pre-Cenozoic normal faulting in the Osgood Mountains, Humboldt Country, Nevada. Geology 8: 594–598

Bettels KH (1989) Gold deposits of the Goldstrike mine, Carlin trend, Nevada. Society of Mining Engineers Preprint 89–158: 14p

Bonham HF (1985) Characteristics of bulk-minable gold-silver deposits in Cordilleran and island-arc settings. US Geol Survey Bull 1646: 821–843

Cline JS, Hofstra AH, Rye RO, Landis GP (1996) Stable isotopes and fluid inclusion evidence for a deep sourced ore fluid at the Getchell, Carlin-type gold deposit, Nevada. PACROFI VI University of Wisconsin at Madison, Extended abstr pp 33–35

Hausen DM (1981) Process mineralogy of auriferous pyritic ores at Carlin, Nevada. In: Hangi House DM, Park WC (eds) Process mineralogy, extractive metallurgy, mineral exploration, energy resources. Metallurgical Society, AIME, pp 271–289

Ghasemipur R, Khoie N (1971) Mineral prospection and a review of the metallogeny of the Takab area. Geological Survey of Iran unpublished report 81p

Ilchik RP, Barton MD (1997) An amagmatic origin of Carlin-type gold deposits. Econ Geol 92: 269–288

Joralemon P (1951) The occurrence of gold at the Getchell mine, Nevada. Econ Geol 46: 267–310
Joralemon P (1975) K-Ar relation of granodiorite emplacement and tungsten and gold mineralization near the Getchell mine, Humboldt Country, Nevada-a discussion. Econ Geol 70: 405–406
Kuehn CA, Rose AW (1992) Geology and geochemistry of wall-rock alteration at the Carlin gold deposit, Nevada. Econ Geol 87: 1697–1721
Kuehn CA, Rose AW (1995) Carlin gold deposits, Nevada: origin in a deep zone of mixing between normally pressured and overpressured fluids. Econ Geol 90: 17–36
Kyazimov RA (1993) Development of technology of noble metals recovery from ores of Zarshuran field, Islamic Republic of Iran, Azergyzyl state company, Baku
Mehrabi B (1997) Genesis of the Zarshuran gold deposit, NW Iran. Unpublished PhD Thesis, University of Leeds, UK
Mohajer G, Parsaie H, Fallah N, Ma'dani F (1989) Mercury exploration in the Saein Dez-Takab. IIMRA Tehran 68p (in Farsi)
Nabavi MH (1976) An introduction to the geology of Iran. Geological Survey of Iran 110 p (in Farsi)
Osterberg MW (1990) Geology and geochemistry of the Chimney Creek gold deposit, Humboldt Country, Nevada. PhD Thesis University of Arizona, Tuscon, USA
Percival TJ, Bagby WC, Radtke AS (1988) Physical and chemical features of precious-metal deposits hosted by sedimentary rocks in the western United States. In: Schafer RW, Cooper JJ, Viker PG (eds) Bulk minable precious metal deposits of the western United States. Geological Society of Nevada, Reno, Nevada, pp 11–34
Phillips GN, Powell R (1993) Link between gold provinces. Econ Geol 88: 1084–1098
Radtke AS (1985) Geology of the Carlin gold deposit, Nevada. US Geol Surv Prof Pap 1267: 124p
Radtke AS, Dickson FW (1976) Genesis and vertical position of fine-grained disseminated replacement-type gold deposits in Nevada and Utah, USA. In: Problems of ore deposition. Proc Fourth IADOG Sym Varna Bulgaria 1974. Sofia Bulgarian Academy of Sciences 1: 71–78
Radtke AS, Rye RO, Dickson FW (1980) Geology and stable isotope studies of the Carlin gold deposits, Nevada. Econ Geol 75: 641–672
Rex DC (1994) K/Ar age determinations of samples from Leg 134. Proc ODP Sci Results 134: 413–414
Rex DC, Guise PG, Wartho JA (1993) Disturbed $^{40}Ar/^{39}Ar$ spectra from hornblendes: Thermal loss or contamination? Chem Geol (Isotope Geosci Sect) 103: 271–281
Roberts RJ (1986) The Carlin story. Nevada Bur Mines Geol Rep 40: 71–80
Rota JC (1987) The Gold Quarry deposit. In: Johnson JL (ed) Guidebook for Field Trips, symposium on bulk mineable resources. Geological Society of Nevada, Reno, pp 271–273
Rota JC, Hausen DM (1991) Geology of the Gold Quarry mine. Ore Geol Rev 6: 83–105
Samimi M (1992) Recognisance and preliminary exploration in the Zarshuran. Kavoshgaran Eng Consultant Tehran (in Farsi)
Seedorff E (1991) Magmatism, extention, and ore deposits of Eocene to Holocene age in the Great Basin-mutual effects and preliminary proposed genetic relationships. In: Raines GL, Lisle RE, Schafer RW, Wilkinson WH (eds) Geology and ore deposits of the Great Basin, Reno. Geological Society of Nevada, pp 133–178
Sha P (1993) Geochemistry and genesis of sediment-hosted disseminated gold mineralization at Gold Quarry mine Nevada. Unpub. PhD Thesis, University of Alabama, USA, 224 p
Silberman ML, Berger BR, Koski RA (1974) K/Ar age relationship of granodiorite emplacement and tungsten and gold mineralization near the Getchell mine, Humboldt Country, Nevada. Econ Geol 69: 646–656
Silberman ML, McKee EH (1971) K/Ar dates of granitic plutons in north-central Nevada. Isochorn/West 1, 15–32
Sillitoe RH, Bonham HF (1990) Sediment-hosted gold deposits: distal products of magmatic-hydrothermal systems. Geology 18: 157–161
Stocklin J (1968) Structural history and tectonics of Iran: a review. Am Assoc Petrol Geol (AAPG) Bull 52: 1229–1258
Taddaion AH (1991) Detailed geochemical prospection in Zarshuran mine area, Takab. Ministry of Mines and Metals Zarshuran gold project 79p (in Farsi)
Thorman CH, Christensen OD (1991) Geologic settings of gold deposits in the Great Basin, western United States. In: Ladira EA (ed) Brazil Gold'91. Balkema, Rotterdam, pp 65–75
Weissberg BG (1965) Getchellite, $AsSbS_3$, a new mineral from Humboldt country, Nevada. Am Mineral 50: 1817–1826
Wilson PN, Parry WT (1995) Characterization and dating of argillic alteration in the Mercur gold district, Utah. Econ Geol 90: 1197–1216
White NC, Hedenquist JW (1990) Epithermal environments and styles of mineralisation: variations and their causes, and guidelines for exploration. J Geochem Explor 36: 445–474